NBS REPORT
6790

FADING CHARACTERISTICS AND BANDWIDTH CAPABILITY FOR WITHIN-THE-HORIZON PROPAGATION AT 1040 AND 9300 MC/S

by

A. F. Barghausen, A. P. Barsis, and R. S. Kirby

NBS

U. S. DEPARTMENT OF COMMERCE
NATIONAL BUREAU OF STANDARDS
BOULDER LABORATORIES
Boulder, Colorado

THE NATIONAL BUREAU OF STANDARDS

Functions and Activities

The functions of the National Bureau of Standards are set forth in the Act of Congress, March 3, 1901, as amended by Congress in Public Law 619, 1950. These include the development and maintenance of the national standards of measurement and the provision of means and methods for making measurements consistent with these standards; the determination of physical constants and properties of materials; the development of methods and instruments for testing materials, devices, and structures; advisory services to government agencies on scientific and technical problems; invention and development of devices to serve special needs of the Government; and the development of standard practices, codes, and specifications. The work includes basic and applied research, development, engineering, instrumentation, testing, evaluation, calibration services, and various consultation and information services. Research projects are also performed for other government agencies when the work relates to and supplements the basic program of the Bureau or when the Bureau's unique competence is required. The scope of activities is suggested by the listing of divisions and sections on the inside of the back cover.

Publications

The results of the Bureau's research are published either in the Bureau's own series of publications or in the journals of professional and scientific societies. The Bureau itself publishes three periodicals available from the Government Printing Office: The Journal of Research, published in four separate sections, presents complete scientific and technical papers; the Technical News Bulletin presents summary and preliminary reports on work in progress; and Basic Radio Propagation Predictions provides data for determining the best frequencies to use for radio communications throughout the world. There are also five series of nonperiodical publications: Monographs, Applied Mathematics Series, Handbooks, Miscellaneous Publications, and Technical Notes.

A complete listing of the Bureau's publications can be found in National Bureau of Standards Circular 460, Publications of the National Bureau of Standards, 1901 to June 1947 ($1.25), and the Supplement to National Bureau of Standards Circular 460, July 1947 to June 1957 ($1.50), and Miscellaneous Publication 240, July 1957 to June 1960 (Includes Titles of Papers Published in Outside Journals 1950 to 1959) ($2.25); available from the Superintendent of Documents, Government Printing Office, Washington 25, D. C.

NATIONAL BUREAU OF STANDARDS REPORT

NBS PROJECT 8370-12-83470 August 15, 1961 **NBS REPORT** 6790

FADING CHARACTERISTICS AND BANDWIDTH CAPABILITY FOR WITHIN-THE-HORIZON PROPAGATION AT 1040 AND 9300 MC/S

by

A. F. Barghausen, A. P. Barsis, and R. S. Kirby

This work was supported by the U. S. Army Signal Research and Development Laboratories, Ft. Monmouth, New Jersey.

U. S. DEPARTMENT OF COMMERCE
NATIONAL BUREAU OF STANDARDS
BOULDER LABORATORIES
Boulder, Colorado

TABLE OF CONTENTS

FADING CHARACTERISTICS AND BANDWIDTH CAPABILITY FOR WITHIN-THE-HORIZON PROPAGATION AT 1040 AND 9300 MC/S

by

A. F. Barghausen, A. P. Barsis, and R. S. Kirby

ABSTRACT

During the early months of 1961 the National Bureau of Standards established a 113 km tropospheric within-the-horizon path in Eastern Colorado in order to investigate propagation characteristics of signals in the 9300 Mc/s range over such a path. Special attention was given to the short-term fading characteristics of the received carrier envelopes, and to the bandwidth capability of the medium. The latter was studied by comparing the amplitude variations of two continuous-wave carriers separated by 100 Mc/s in the 9300 Mc/s frequency range. Separate antennas were used in transmission and reception of the two carriers; consequently, the results include the effects of space diversity. In addition to studying the correlation of carrier envelopes as a measure of the bandwidth capability, an analysis was also made of the distribution of the carrier amplitude ratios, which is related to the correlation coefficient, and is believed to be a better indicator, at least for line-of-sight paths, of selective fading phenomena.

Short-term fading in the 9300 Mc/s range can be characterized in terms of "prolonged space-wave fadeouts," which have previously been observed and described for lower carrier frequencies over this and similar paths. Fadeouts appear to be well correlated in time of occurrence on the two frequencies 9250 and 9350 Mc/s. The fading durations range from a few tenths of a minute to 10 minutes, and the maximum observed depth was 25 db below the median of a five-day observation period.

The cross-correlation coefficient of instantaneous carrier envelopes separated by 100 Mc/s had an overall value of 0.91, as determined by sampling of the carrier amplitudes at the rate of one per second. The standard deviation of the amplitude ratios averaged 0.76 db, with a maximum hourly value of 1.81 db. These results support the feasibility of wide-band modulation techniques for within-the-horizon paths if evaluated by amplitude variations of discrete frequencies within the bandwidth of interest. Sufficient margin in transmitter power has to be provided to allow for the short-term signal variations observed.

Supporting measurements on 1040.1 Mc/s over this path confirmed previously established fadeout characteristics with regard to diurnal variations, depth, and duration of fadeouts. However, the distribution of hourly median signal levels on this frequency showed a much larger month-to-month variation than had previously been observed over this path. This is attributed to the small sample size available in the current measurement series.

1. INTRODUCTION

The Central Radio Propagation Laboratory of the National Bureau of Standards, in cooperation with the U. S. Army Signal Research and Development Laboratories, has carried out a study of the bandwidth capabilities of the medium for within-the-horizon transmission paths at low grazing angles. Tests were carried out on a 113 km path, using the summit of Cheyenne Mountain near Colorado Springs, Colorado, as the transmitting terminal, and a site on the eastern plains near Karval, Colorado, as the receiving terminal. Unmodulated carrier frequencies at 9250 and 9350 Mc/s were used with supplementary transmissions at 1040.1 Mc/s. The primary

objectives of this study are to determine both fading and bandwidth characteristics applicable to line-of-sight propagation paths up to 800 km long. It was not considered feasible to use the same antenna for the two frequencies in the 9300 Mc/s range; therefore, the results also contain the effects of space diversity with about 30 wavelengths separation between antenna centers.

It has been customary to assume that coherence over a finite frequency band is maintained as long as the cross-correlation coefficient of the signal levels at the limits of the band is in excess of approximately 0.5. So far this type of analysis has largely been applied to beyond-the-horizon propagation where the short-term fading can often be characterized by a single-parameter distribution, such as the Rayleigh distribution. However, it is also possible to study the instantaneous amplitude variations of the signals at the limits of the band. An analysis of the changing ratios of these amplitudes provides another indication of the bandwidth capability in terms of the selective fading components only and this should be especially useful for predicting the performance of an amplitude-modulated system.

Let x represent the varying signal in one part of the band to be investigated and y another signal in the same band, but displaced from x by a constant amount in frequency. Then, assuming that x and y are expressed in decibels and that each are normally distributed, the following relation may be written:

$$\sigma_{x-y}^2 = \sigma_x^2 + \sigma_y^2 - 2\rho\sigma_x\sigma_y \qquad (1)$$

The first term, σ_{x-y}^2, represents the variance in the amplitude ratios of the two signals, which in this case are instantaneous values. The variance of the individual signals is expressed by σ_x^2 and σ_y^2. The correlation between instantaneous values of x and y is expressed by ρ.

In determining bandwidth capability, the real interest lies in the investigation of selective fading, or the tendency for one signal to fade independently relative to the other. The amount of non-selective fading, or the tendency for the two signals to fade in unison, is of no concern here. However, all fading, selective and non-selective, is included in the terms σ_x^2 and σ_y^2 of (1), whereas the term σ_{x-y}^2 contains only the selective fading tendency. Thus the relationship between σ_{x-y}^2 and ρ contains a consideration of the non-selective fading, and it follows that ρ itself is influenced by non-selective fading.

This characteristic can be demonstrated by an example, which is based on the use of a receiver with AGC action, although the argument could be presented as well without consideration of AGC. Assume a carrier, amplitude modulated by a sine wave. This results in three distinct signals: the carrier, the upper side band, and the lower side band. If this is passed through a receiver with AGC, the input to the demodulator will have the unison, or non-selective fading removed, at least to an extent depending on the capability of the AGC circuit. The remaining fading characteristics are those contained in each of the two signals which are independent of each other. If the AGC is the exact inverse of the carrier amplitude, the remaining fading will be entirely restricted to the two side bands.

The variance of the selective fading as expressed by σ_{x-y}^2 will be independent of the amount of non-selective fading, whereas ρ depends not only on σ_{x-y}^2, but also on the non-selective fading represented by σ_x^2 and σ_y^2. Thus ρ may have various values for a fixed value of σ_{x-y}^2. It is also possible to assume two distinct propagation mechanisms, and identify the non-selective fading with a slowly varying component responsible for space-wave fadeouts and similar phenomena, whereas the selective fading component is identified by a

smaller "scatter" component, which varies more rapidly, and is superimposed on the non-selective variations. This model is a reasonable assumption resulting from the analysis of data previously obtained at lower carrier frequencies over this and similar paths [Janes and Wells, 1955].

For the present data, correlation coefficients between instantaneous values of signal strength (expressed in decibels) and the ratio of instantaneous signal strength values were estimated by analyzing the records obtained at each carrier frequency for periods ranging from several minutes to several hours. Correlation coefficients and ratios obtained are a function of the frequency separation between carriers as well as other propagation variables. Therefore, if the correlation is high and the ratio has only a small dispersion, this indicates that the signal components are essentially in agreement and little or no distortion is expected over the entire band. Conversely, if the correlation is low, and the dispersion in the ratio is large, distortion is present and the useful modulation bandwidth must be reduced to maintain coherence.

Methods utilizing the concepts of geometrical optics may be used to determine the transmission loss for line-of-sight paths during most transmission periods. However, additional phenomena, such as reflections from layers and trapping of the signal in ducts, must be taken into account. Although they may produce signal enhancement on beyond-the-horizon paths, simultaneous defocusing of the energy within the horizon has also been observed, resulting in fading of the space-wave fadeout type [Bean, 1954]. To ascertain the effects of these prolonged space-wave fadeouts the experimental data for both frequency ranges have also been analyzed in terms of the time distributions of fade durations, the depth of fades, and the frequency of fadeout occurrence.

2. PATH PARAMETERS AND EQUIPMENT CHARACTERISTICS

2.1. Transmission Path

The experimental investigation covered by this report was performed over a 113 km line-of-sight transmission path extending from the summit of Cheyenne Mountain, near Colorado Springs, Colorado, eastward over relatively flat terrain, to Karval, Colorado. This path has been described previously [Barsis, Herbstreit, and Hornberg, 1955]. A detailed terrain profile, plotted on the basis of a 4/3 earth's curvature is shown in Fig. 1 and the various path parameters are given in Table 1 below.

TABLE I

Transmitter Site:

Location:	Cheyenne Mountain, Colorado	
Geographical Coordinates:	38° 45' 50.4" N 104° 51' 50.4" W	
Elevation:	2,670 m above mean sea level	
	1040.1 Mc/s	9250-9350 Mc/s
Nominal Transmitter Power:	20 w	100 w
Parabolic Transmitting Antenna Diameter:	3.05 meters	0.74 meters
Transmission Line Losses:	1.2 db	1.65 db
Half Power Antenna Beamwidth:	6.5°	3.25°
Antenna Gain (Above Isotropic):	28 db	34 db
Modulation:	Continuous Wave	
Polarization:	Horizontal	

TABLE I (Continued)

Receiver Site:

Location:	Karval, Colorado	
Geographical Coordinates:	36° 37' 55.2" N 103° 34' 19.2" W	
Elevation:	1,543 m above mean sea level	
	1040.1 Mc/s	9250-9350 Mc/s
Parabolic Receiving Antenna Diameter:	3.05 meters	0.74 meters
Transmission Line Losses:	1.6 db	0.8 db
Half Power Antenna Beamwidth:	6.5°	3.25°
Antenna Gain (Above Isotropic):	28 db	34 db
Distance to Transmitting Site:	113 km	
Grazing Angle:	3.6 milliradians	

Fig. 2 contains photographs of the transmitting installation on Cheyenne Mountain, and Fig. 3 contains photographs of the Karval receiving location.

The parabolic antennas for the 9300 Mc/s propagation studies at the receiving location were mounted 2.6 meters above the ground to coincide with the maximum of the "first lobe" obtained by calculation of the smooth earth interference pattern which results between the direct and ground reflected rays for within the line-of-sight paths. The calculated lobe patterns for all three operating frequencies are shown on Fig. 4, based on an atmosphere with a constant refractivity gradient and a surface refractivity value N_s = 280 N-units. This represents an estimate of average conditions for the winter months in Eastern Colorado [Bean and Horn, 1959]. For the 2.6 meter

receiving antenna elevation used, variations in the refractive index gradient will have very little effect on the relative phase between direct and ground reflected rays. The "first lobe" maximum shifts by approximately 0.6 meters for a change in the refractivity from 240 to 300 N-units. At the fixed antenna height used the variation in transmission loss over this range of refractivity is 0.5 decibels. Other assumptions for these calculations were smooth level terrain in the foreground of the receiving antenna with a reflection coefficient of -0.9.

2.2. 9300 Mc/s Transmitting and Receiving Equipment

The 9300 Mc/s transmitting and receiving equipment was furnished by USARDL and modified for the purpose of this experiment.

The two transmitters, operating at 9250 Mc/s and 9350 Mc/s, employed BLC Z-2J51 magnetrons operating in a continuous wave mode with an average power output of 100 watts. The maximum frequency range of this type of magnetron is from 8500 to 9600 Mc/s. The output frequency was maintained by means of a discriminator network which provided the desired AFC voltages to automatically tune the magnetrons by means of a motor attached to a tuning shaft on each cavity. A 21 db directional coupler was used between the transmitter and antenna to divert a small portion of the magnetron output to the automatic frequency control unit.

The output power was fed to two 0.74 meter diameter parabolic antennas, mounted side by side, by means of standard RG-52/U waveguide. Horizontal polarization was used throughout the tests.

The output power of each transmitter was continuously monitored by recording the current developed through a 1N23-B crystal detector. The output power of the magnetron was coupled to the crystal through

a directional coupler and precision variable attenuator combination of approximately 40 db. The variations in current were recorded on a strip chart recorder. The full-scale or reference value on the recorder was determined by using a Hewlett-Packard Type 434-A calorimetric power meter.

The receivers used at both microwave frequencies have identical characteristics. The incoming signals are mixed with a local oscillator signal in a "magic T" to produce an intermediate frequency of 100 Mc/s. The local oscillator frequency is generated by a type 2K25 klystron. The frequency of the klystron is controlled by variations in voltage on its repeller supply obtained from a ratio frequency discriminator at the output of the intermediate frequency amplifier. Since the two carriers are separated by a frequency difference of 100 Mc/s and the intermediate frequency is also 100 Mc/s, the local oscillator of one carrier is above the signal frequency and the other is below the signal frequency.

The output of the 100 Mc/s IF amplifier chain is detected and amplified to drive a strip chart recorder. In addition, the detector output is fed directly to a multi-channel magnetic tape recorder.

To obtain a reasonably linear relationship between voltage output and signal input, automatic gain control was not used in the intermediate frequency amplifier. When necessary, fixed values of attenuation were inserted at the receiver input to prevent overloading due to high signal levels. Both the transmitters and receivers, were powered from 115 v, 400 cps gasoline engine-driven generators.

Table II lists the operating characteristics of the microwave receivers.

TABLE II

Radio Frequency:	9250 and 9350 Mc/s
Local Oscillator Frequency:	9150 and 9450 Mc/s
Intermediate Frequency:	100 Mc/s
Bandwidth:	7 Mc/s (3 db down)
Sensitivity:	-63 dbm
Dynamic Range:	>32 db

2.3. 1040.1 Mc/s Transmitting and Receiving Equipment

The 1040.1 Mc/s transmitter has a maximum power output of 30 watts. The driver unit consists of a 10 Mc/s crystal oscillator having a long term frequency stability of one part in 10^8 per day.

The receiver is a double super-heterodyne type using a pre-selector input coaxial cavity to insure adequate image signal rejection. A coaxial type crystal mixer using a 1N23B crystal serves as the first stage. The local oscillator signal is obtained by multiplication from a 10 Mc/s oscillator which also has a long term frequency stability of one part in 10^8 per day. The first intermediate frequency is 39.9 Mc/s and the second is 100 kc/s. The output signal is then detected and recorded on a strip chart recorder and on magnetic tape. Again, automatic gain control was not used in the receiver to insure a reasonably linear voltage output versus signal input.

Table III lists the operating characteristics of the 1040.1 Mc/s receiver.

TABLE III

Radio Frequency:	1040.1 Mc/s
Local Oscillator Frequency:	1080 Mc/s
1st IF:	39.9 Mc/s
2nd IF:	100 kc/s
1st IF Bandwidth:	1 Mc/s (3 db down)
2nd IF Bandwidth:	1.2 kc/s (3 db down)
Sensitivity:	-120 dbm
Dynamic Range:	>30 db
Noise Figure:	13 db

3. RESULTS OF MEASUREMENTS

3.1. Variability of Hourly Medians

In the analysis of transmission loss or field strength measurements it has been found convenient to distinguish between short-term and long-term variations and fix the dividing line arbitrarily at the period of one hour. In this way, each hour of measurements may be characterized by one single parameter, usually the hourly median of transmission loss, and the variability of the hourly medians investigated as a function of the time of the day, the season of the year, and of path parameters [Norton, Rice, and Vogler, 1955]. This procedure is also useful in coordinating all measured data in a data pool, which in turn serves as a basis for communication circuit analysis and performance predictions [Rice, Longley, and Norton, 1959]. The short-term variations within each hour may then be treated separately according to the path characteristics.

Fig. 5 shows the cumulative distribution of hourly medians measured on 1040.1 Mc/s during the three recording periods. The

abscissa scale is in percent of all hours, and the ordinate scale is in decibels of basic transmission loss, L_b. Basic transmission loss is the ratio, expressed in decibels, between the power radiated from an assumed isotropic transmitting antenna and the power received by an assumed isotropic receiving antenna [Norton, 1953 and 1959]. It is related to the total transmission loss, L, which is the ratio of power delivered by the transmitter to the power available at the receiver input terminals, by the following expression, where all terms are in decibels:

$$L_b = L + G_p - L_t - L_r \qquad (2)$$

Here, L_t and L_r are the transmission line losses at the terminals, and G_p is the path antenna gain relative to an isotropic radiator. It is assumed that for a line-of-sight path of the type studied the free-space antenna gains are fully realized, $G_p = G_t + G_r$, and that any loss in antenna gain (sometimes called aperature-to-medium coupling loss) may be neglected. Furthermore, in the frequency ranges used and for parabolic reflectors, any antenna circuit losses are usually negligible and may be neglected, so that system loss and transmission loss as used by Norton [1959] are equivalent.

Antenna gains were either measured by comparison with standard dipoles, or they were assumed from antenna specifications. Transmission line losses were measured, and the received signal was calibrated by standard signal generators using the substitution method.

Inspection of Fig. 5 shows a very marked change in the signal level between the January and the March period. This may not be significant due to the relatively small sample (number of hours) in each case; it is quite likely that a period of high signal (small transmission loss) was accidentally chosen for the March measurements.

For each curve the period, number of hours, and the overall median value is indicated.

A similar study is shown on Fig. 6 for the two X-band frequencies (9250 and 9350 Mc/s). Here the increase in signal strength between January and March is still evident, but to a smaller degree. The distributions for the two X-band frequencies are relatively close together, as expected. On each of the figures the calculated values of basic transmission loss, taken from Fig. 4 at the appropriate antenna heights, are also shown for comparison.

From Figs. 5 and 6, the following table may be compiled listing overall medians and long-term variability. The latter is here defined as the 1-99% range of hourly medians; i.e., the db difference in levels exceeded by 1% and by 99% of all hourly medians within the specified measurement period.

TABLE IV

Overall Medians and Long-Term Variability in Basic Transmission Loss for Cheyenne Mountain - Karval Propagation Path

Period	1040.1 Mc/s	9250 Mc/s	9350 Mc/s
	Overall Medians, db		
January 18-24	144.6	155.5	154.5
January 31-February 1	143.9	153.1	152.6
March 6-10	133.9	150.2	149.3
	1% to 99% Range of Hourly Medians, db		
January 18-24	10.0	15.5	14.2
January 31-February 1	15.7*	10.0*	7.5*
March 6-10	20.9	9.3*	8.3

* Extrapolated

In previous years, transmission loss measurements were made over the same path using frequencies of 100, 192.8, 230, and 1046 Mc/s. At that time the dipole antenna on top of the Karval tower (see Fig. 3) was used for receiving the 1046 Mc/s signal. This dipole is 13 meters above ground. Overall monthly median basic transmission loss values for the period February 1952 to August 1953 ranged from 143 to 152 db, when allowance is made for the antenna elevation difference between those measurements and the current data. The 1% to 99% range of hourly medians for the same period was between 11 and 16 db. These data, including some height gain measurements, have not been formally published except for some samples contained in NBS Circular 554 [Barsis, et al, 1955].

The current 1040.1 Mc/s data fit in fairly well within the results previously recorded in 1952 and 1953, except for the high signal (low overall median transmission loss) and the large range of the medians during March; such differences may be attributed to the short recording periods involved in the present measurements.

Although the overall basic transmission loss medians on 9250 and 9350 Mc/s follow the same trend as the 1040.1 Mc/s data with higher fields in March, the 1 to 99% range of the hourly medians is smaller for the March period as compared to January, and thus follows a trend opposite to the one of the 1040.1 Mc/s data in this respect.

3.2. Short-Term Signal Variations (Space-Wave Fadeouts)

The short-term (usually within-the-hour) signal variations over within-the-horizon paths have been termed "space-wave fadeouts" [Bean, 1954]. They are somewhat different phenomena from the short-term Rayleigh distributed signal variations usually observed

over beyond-the-horizon tropospheric or ionospheric propagation paths. Whereas fading on beyond-the-horizon paths is characterized by relatively fast amplitude variations to which a definite fading rate may be assigned, space-wave fadeouts are much slower and more irregular amplitude variations which are not easily represented or approximated by a simple distribution function. Space-wave fadeouts are presumably caused by defocussing of the radio frequency energy by refractive index gradients or by vector addition of a limited number of specular field components due to reflections from shifting atmospheric layers.

As previously defined, a space-wave fadeout is presumed to exist whenever the received carrier level drops to at least 5 db below a specified reference value for a given minimum time period. In Bean's original work [1954] the minimum fadeout duration considered was one minute, and the specified reference level was the monthly basic transmission loss median. In additional work [Barsis and Johnson, 1961], expanded time scales of the recording charts permitted accurate determination of 0.1 minute fade durations, and other reference levels were used for comparative studies.

For the data investigated here, the "overall" medians for the individual recording periods shown on Table IV were used as reference levels, and the minimum measurable fadeout duration was 0.1 minutes. Recording chart samples for all three frequencies are shown on Figs. 7 and 8, each comprising 30 minutes of data. For the afternoon hour represented by the sample on Fig. 7, no space-wave fadeouts at all were found, as the carrier level excursions do not extend to 5 db below the reference level. The relatively small and rapid amplitude variations noticeable on the signal traces are probably due to a weak scatter component superimposed on the much stronger space-wave field, and not strong enough to have any influence on the analysis of space-wave

fadeouts conducted here. As expected, these rapid variations are more evident on the X-band frequencies than at 1000 Mc/s. Although they are of little concern in the study of space-wave fadeouts, they will have some effect on the correlation between instantaneous carrier level intensities.

Similar chart samples for a late evening hour are shown on Fig. 8. Here, space-wave fadeouts are present, and they have been indicated on the three charts wherever they occur. Space-wave fadeouts are slow carrier-level variations of relatively large amplitude, on which again small "scatter" components are superimposed. For this sample, the traces for 9250 and 9350 Mc/s appear to be well correlated. The space-wave fadeouts on 1040.1 Mc/s are much longer than the ones on the two X-band frequencies.

When interpreting fadeout statistics one should recognize that several fadeouts to the 10 db or deeper levels may occur during one single 5 db fadeout. Also, the difference in the overall median reference levels may result in fadeouts appearing only on one of the two X-band records during the same time period. Both of these facts are demonstrated on Fig. 8, where several short 10 db fadeouts occur on 9350 Mc/s during one long 5 db fadeout, and where no 10 db fadeouts at all are observed on this portion of the 9250 Mc/s record.

For a study of the diurnal variations of fadeout characteristics, fadeout levels were referred to the overall median of the respective recording period (January and March). Fadeout incidence is defined as the number of times the signal dips below a given level for at least 0.1 minutes. Fadeout time is the total time within a recording period the signal stays at or below a given level. Fadeout incidence and fadeout level were determined visually from the strip-charts as demonstrated by the example on Fig. 8. In order to evaluate diurnal

variations, the "time block" concept was used [Norton, Rice, and Vogler, 1955] where the day is divided into 4 time blocks for each of the winter and summer seasons. The data obtained over this path only applies to the four winter time blocks, as follows:

Time Block 8	0000 - 0600
Time Block 1	0600 - 1300
Time Block 2	1300 - 1800
Time Block 3	1800 - 2400

Mountain Standard Time has been used throughout.

On Fig. 9, fadeout time in percent of all hours and fadeout incidence normalized to the number of fadeouts per hour are plotted for the four time blocks and for the 5 and 10 db fadeout levels. Fadeout incidence is substantially greater for the higher frequencies than for 1040.1 Mc/s; whereas the fadeout times are more comparable. This is due to the generally shorter durations of the individual fadeouts in the 9300 Mc/s frequency range, combined with the much greater fadeout incidence. Clearly, the minimum fadeout incidence as well as duration occurs for Time Block 2, which corresponds to the afternoon hours, and maximum fadeout incidence and duration occurs at night. This is typical of a region with a continental climate, which favors the formation of ground-modified layers at night only; the observed diurnal trend agrees quite well with previous data obtained for the same path on 1046 Mc/s [Bean, 1954; Barsis and Johnson, 1961].

Fig. 9 shows a maximum fadeout time of 20% for 5 db fadeouts and 6.5% for 10 db fadeouts, both on 9250 Mc/s and for the evening hours (Time Block 3). This means that during these hours the signal can be expected to remain substantially below its overall median value

for an amount of time which may be operationally quite significant. This reduction in available signal level requires an appropriate margin in the equipment design.

Fig. 10 shows cumulative distributions of fadeout durations for the three frequencies. Each curve is labelled with the fadeout level and the number of fadeouts used; as an example the solid curve on the upper graph (for 1040.1 Mc/s) means that of the total 104 5-db fadeouts observed, 90% had a duration of at least 0.39 minutes, 50% of at least 4.2 minutes, and 10% of at least 26 minutes. Equivalent values may be read from the other curves. In general, the cumulative distributions of fadeout durations are approximately normal if plotted versus the logarithm of the duration [Barsis and Johnson, 1961]. Irregularities shown on Fig. 10 are probably due to the limited amount of data available. One would also expect a closer resemblence of the two sets of curves for 9250 and 9350 Mc/s; this may also be due to the limited sample size available.

Table V shows comparative figures for fadeout durations exceeded for 10, 50, and 90 percent of all fadeouts at the various levels relative to the overall median for the appropriate 5-day recording period. In the interpretation of these data it is necessary to keep in mind that the half-power antenna beamwidths are different for the two frequency ranges, amounting to 6.6° for 1040.1 Mc/s, and approximately 3° for 9250 and 9350 Mc/s. It is not possible on the basis of the data reported here to separate the effect of frequency from the effect of antenna beamwidth when studying fadeout characteristics.

TABLE V

Fadeout Duration Statistics

(a) Duration in minutes exceeded by 10% of all fadeouts.

Fadeout Level, Decibels	Carrier Frequency, Mc/s		
	1040.1	9250	9350
5	26	5.9	5.6
10	19	3.6	3.4
15	24	3.2	2.2
20	7.4	3.3	1.35
25	4.2	3.4	0.94

(b) Duration in minutes exceeded by 50% of all fadeouts (median fadeout duration).

Fadeout Level, Decibels	Carrier Frequency, Mc/s		
	1040.1	9250	9350
5	4.2	0.83	0.78
10	1.6	0.73	0.72
15	1.2	0.63	0.54
20	0.72	0.49	0.42
25	0.42	0.46	0.30

(c) Duration in minutes exceeded by 90% of all fadeouts.

Fadeout Level, Decibels	Carrier Frequency, Mc/s		
	1040.1	9250	9350
5	0.39	0.16	0.13
10	0.22	0.15	0.16
15	0.20	0.135	0.125
20	0.14	0.10	0.12
25	0.16	0.105	<0.10

In general, fadeout durations are less for the higher frequencies, but the ratio of durations at 1040.1 and 9300 Mc/s tends to equalize for short fadeouts. This is probably due to the arbitrary cut-off in the definition of a fadeout, which was restricted to a duration of at least 0.1 minutes due to the analysis techniques employed. This causes an apparent convergence of the values of higher percentages like 90 or greater. However, even at the low percentage values, the ratio of fadeout durations for the 1000 and the 9000 Mc/s range is smaller for the deeper fadeout levels.

Differences in the results for the 9250 and 9350 Mc/s data may be ascribed to the limited sample size, as before. More refined recording and analysis methods may also be expected to provide better results. However, the material presented here gives at least a qualitative indication of the distribution of fadeout durations in the two frequency ranges, and indicates the number of times when outages due to fadeouts may be expected to occur on communication links utilizing paths of this type.

Still another, somewhat more general type of fadeout analysis, is shown in Figs. 11, 12, and 13. Here, the analysis is made at a number of specific levels above as well as below the reference level (overall median for the recording period), and the graphs result in the distributions of fadeout durations and duration of the time periods during which the signal exceeds specific levels. The asymptotic extensions downward of the curves shown would result in the instantaneous signal level distributions.

These graphs are shown for each of the three frequencies using the recording period March 6-10, 1961. The abscissa scale is in terms of percentage of the <u>total</u> time of the recording period, during which the signal either exceeds or is below the levels indicated by the

curve designation for at least the time period in minutes shown by the ordinate. As an example, on Fig. 13(b) for 9350 Mc/s, fade durations of one minute or longer are observed for 10% of the total time at the basic transmission loss level of 152.5 db. Following the same abscissa value up, it is seen that fade durations of 12.5 minutes or longer would occur for the same percentage of the total time at the 151.0 db basic transmission loss level. If the interest of the user concerns fades of one minute or longer, the one minute ordinate value indicates such fades for 3.3% of the total time at the 155 db level, 10% of the time at the 152.5 db level, 17.5 db of the time at the 151 db level, and 37% of the time at the 149.3 db level, which is the overall median for the period concerned. Similarly, on the right-hand side of the graphs, corresponding values of signal values exceeded are read; e.g., the median level is exceeded for periods of at least one minute during 34% of the total time, etc. It is quite obvious that the two "median" curves have to converge to a common point for very short durations of fades or signal exceeded, namely the 50% abscissa values.

As shown by the examples, these graphs may be used to determine the percentage fadeout time at various arbitrary levels and for any desired minimum fade duration. Thereby additional means of estimating the influence of fadeouts on the performance of a system are provided for paths of this type.

3.3. Correlation of Hourly Medians

It was expected that the carrier envelopes would exhibit similar characteristics at the two X-band frequencies in terms of transmission loss levels and dispersion of instantaneous values, inasmuch as the transmission paths were almost identical. Because of physical limitations in placing the two transmitting and the two receiving antennas

adjacent to each other the actual separation between feed points was on the order of 30 wavelengths. These antennas were arranged so that the paths were parallel during the January run, but crossed during the March run. Fig. 6 and Table IV show the general similarity of these results, but also show some differences, some of which may be attributed to the physical separation. Fig. 14 shows the same type of information relative to comparative values of hourly median values of basic transmission loss. Each circle on Fig. 14 represents both medians observed simultaneously on 9250 Mc/s and 9350 Mc/s during January. The crosses represent similar values for the March run. It is seen that the January data are much more scattered and generally correspond to higher transmission loss values in agreement with the appearance of the distribution graphs of Fig. 6.

The concept of correlation is more or less restricted to normally distributed random variables. As it has been found in the case of tropospheric propagation measurements that hourly median transmission loss values (representing logarithms of field strength) have a greater tendency to be normally distributed than the corresponding absolute values of field strength (or receiver input voltage), the correlation concept is more meaningful if transmission loss values are used. Tests have shown that usually no large difference exists in the estimates of correlation coefficients when field strength values are expressed either as voltages, or as logarithms of voltage ratios (decibels).

For the data shown in Fig. 14, sample correlation coefficients of the hourly median basic transmission loss values and their 95% confidence limits based on the number of hours of data have been calculated in accordance with established statistical methods (see, for instance, Bennett and Franklin [1954]). They are shown in

Table VI, below. The possibility of serial correlation between successive hours has not been considered in determining the confidence bands. If such correlation exists the consequence would be somewhat larger bands.

TABLE VI

Correlation of Hourly Median Basic Transmission Loss Values
Cheyenne Mountain - Karval Path, 9250 and 9350 Mc/s

Time Period	Number of Hours	Sample Correlation Coefficient	95% Confidence Limits Lower	Upper
January, 1961	114	0.712	0.607	0.792
March, 1961	50	0.877	0.791	0.928
Both Combined	164	0.800	0.738	0.849

Similar studies were made for the correlation coefficient of hourly median basic transmission loss values measured simultaneously on 1040.1 Mc/s and either one of the X-band frequencies. The resulting sample correlation coefficients are much lower, ranging from 0.645 for 1040.1 versus 9250 Mc/s in March down to 0.251 for 1040.1 versus 9350 Mc/s in January.

3.4. Correlation of Instantaneous Signal Levels, and Signal Ratios

Correlation of the instantaneous values of transmission loss observed simultaneously on the two frequencies has much more bearing on the bandwidth capabilities than does correlation of hourly medians. For this analysis, the 9250 and 9350 Mc/s data were recorded in the field on magnetic tape together with appropriate timing signals for

identification. The tapes were analyzed in the laboratory using a digitizing process, where transmission loss values were automatically read off the magnetic tape at one-second intervals and punched on paper tape. The paper tape was fed into electronic data processing equipment, and correlation coefficients and other parameters were obtained by appropriate programming. The programs also allowed for the determination of serial correlation coefficients of the individual carrier envelopes at various lags in order to obtain estimates of the confidence intervals for the cross-correlation coefficients.

Another method for analyzing the variations in instantaneous amplitudes has been developed specifically for this study, and it has some inherent advantages over the correlation analysis. This method takes into account the AGC action of a receiver and considers variations as they are more typically characterized at the input to the receiver demodulator. A single AGC voltage is usually developed in the receiver and applied to preceding stages so the gain varies inversely to the input R-F signal. The result is that most of the signal variations have been removed at this point, but of course variations from one part of the baseband relative to another remain. It is quite probable that the ratio of signal amplitudes of two separate signals observed at the R-F input will represent the ratios as they appear at the demodulator, and the dispersion of these ratios may turn out to be a more consistent indicator of the bandwidth capability of the system than will correlation studies.

A comparison of these two methods of analysis under different fading situations can be used to demonstrate the advantage of the latter. Suppose in one case deep fading is occurring on the transmission path and that there is a random component on each of two signals in the baseband which is dissimilar. This may be interpreted as two separate

propagation mechanisms acting on the transmitted signal. In another case let all of the fading that occurs be due to this same random component, in which case only one propagation mechanism is thought to be present, and the fading range will be considerably reduced. The AGC action will act on these two situations in such a way that both types of signal will exhibit almost identical characteristics at the input to the demodulator. A study of the dispersion in ratios of instantaneous envelope amplitude of the two signals observed simultaneously will show the same characteristics in either case, but correlation of instantaneous values of transmission loss will differ being higher when the propagation mechanism producing a large fading component common to both signals is present.

In the analysis of signal ratios the algebraic difference in instantaneous transmission loss is taken as a measure of this ratio for any instant of time. Simultaneous pairs of values were tabulated for the 9250 and 9350 Mc/s recordings for 16 one-hour sample periods between March 6 and 9, 1961. The signal ratios, expressed in decibels, are shown for all sample periods in Figs. 15 through 18. In these plots positive decibels indicate the situation in which the 9350 Mc/s signal is the stronger.

Estimates of the cross-correlation coefficient of the carrier envelopes and the standard deviation of individual carrier envelopes with their decibel ratio are shown on the charts for each sample period. Variations in the decibel ratio tend to be greatest when the standard deviations of the individual signals are large; i.e., when the deep-fading mechanism is thought to be present.

It becomes readily apparent from examining Figs. 15 through 18 that the correlation coefficients tend to approach unity when the deep-fading propagation mechanism is present and the carrier envelope

variations are large. Equation (1) in Section 1 shows how the variances of the individual carrier envelopes are used in determining the estimates of the correlation coefficients.

Values of transmission loss for the two signals observed during the same 16 one-hour periods shown in the ratio studies on Figs. 15 through 18 are shown on Figs. 19 through 22. The points on these cross plots represent instantaneous values of transmission loss in db. Although the evaluation of the statistical parameters was based on the data digitized at the rate of one per second as explained above, only every tenth point was plotted on these graphs for the sake of clarity. As on Figs. 15 through 18, the same estimates of the correlation coefficient, r, the standard deviation of the 9250 Mc/s values, s_x, the 9250 Mc/s values, s_y, and of the difference in transmission loss (the ratio) s_{x-y} are tabulated on each plot. Since the maximum fading rates encountered were appreciably greater than one per second, the one-second interval is believed to represent an adequate sampling rate for the purpose of this analysis.

The signal-ratio graphs (plotted in decibels) show very little variation for the first two and one-half hours of data (March 6, 2000-2230 M.S.T.; see Fig. 15). The "spikes" appearing at some places in the record are probably due to "noise," i.e., errors in the magnetic tape or in the digitizing process. At about 2230 on March 6, the dispersion in the distribution of ratios of the two carrier envelopes increased significantly, with individual ratios ranging to about plus or minus 6 db during the following hour. This event coincides with the occurrence of space-wave fadeouts.

During the morning hours of March 7, the dispersion in the ratios are again small (see Fig. 16), and the individual signal records show no fadeouts. Also of interest are the runs shown on Fig. 17;

dispersions are again greater for the hour 1200-1300 on March 9, and the following hours on this day show small, almost cyclic variations in the signal ratios having a period of about one minute. Larger dispersions again appear on Fig. 18 for the hour 0500-0600 on March 10; this hour is again characterized by a number of space-wave fadeouts, but only to less than the 10 db level.

Examination of Figs. 19 through 22 shows that the hours during which the dispersion in the ratios of the two signals is large also tend to be characterized by a much greater spread of the individual transmission loss values, although there appears to be high correlation of these instantaneous transmission loss values for almost every one of the hours analyzed.

The cumulative distribution of the transmission loss values for the individual signals and of their ratios have been compiled and plotted for each of these 16 hours analyzed in detail. The standard deviation of all these distributions are listed on Table VII, together with other pertinent data.

As noted before, estimates of the standard deviations of the transmission loss values for the individual carriers are denoted as s_x and s_y, for 9250 and 9350 Mc/s respectively, and the estimate of the standard deviation of the signal ratios expressed in decibels is denoted s_{x-y}. Estimates of the sample correlation coefficients are denoted by r, and the table also shows the number of the run corresponding to the graphs on Figs. 15 through 22, the date and time of the day, and the observed fadeout statistics when applicable. The distributions of the instantaneous transmission loss levels within each hour are not shown separately on graphs as all distributions are nearly normal and may be represented by their standard deviations s_x and s_y. All standard deviations and correlation coefficients used here are

TABLE VII

Statistics of Instantaneous Transmission Loss Values

Run No.	Date Mar. 1961	Mountain Standard Time	Standard Deviations in Decibels			Correlation Coefficient	Time Block	Fadeout Incidence					
			9250 Mc/s	9350 Mc/s	Ratio			9250 Mc/s			9350 Mc/s		
			s_x	s_y	s_{x-y}	r		5 db	10 db	15 db	5 db	10 db	15 db
1	6	2000-2100	1.35	1.29	0.28	0.979	3	-	-	-	-	-	-
2	6	2100-2200	1.06	1.01	0.33	0.952	3	-	-	-	-	-	-
3	6	2200-2300	3.25	3.97	1.13	0.971	3	8	-	-	12	-	-
4	6	2300-2400	2.98	3.38	1.81	0.846	3	25	5	-	24	10	1
5	7	0000-0100	2.56	2.86	1.14	0.918	8	21	4	-	18	5	-
6	7	0600-0700	0.51	0.53	0.35	0.772	1	-	-	-	-	-	-
7	7	0700-0800	0.44	0.47	0.41	0.587	1	-	-	-	-	-	-
8	7	0900-1000	0.31	0.27	0.26	0.616	1	-	-	-	-	-	-
9	9	0200-0300	0.96	1.08	0.31	0.960	8	-	-	-	-	-	-
12	9	1200-1300	1.28	1.85	0.85	0.915	1	-	-	-	-	-	-
13	9	1300-1400	1.19	1.10	0.71	0.812	2	-	-	-	-	-	-
14	9	1500-1600	0.63	0.58	0.43	0.748	2	-	-	-	-	-	-
15	9	2000-2100	0.98	0.99	0.41	0.915	3	-	-	-	-	-	-
16	9	2100-2200	1.00	1.25	0.64	0.863	3	-	-	-	-	-	-
17	10	0500-0600	1.90	1.82	0.86	0.894	8	17	-	-	10	-	-
18	10	0800-0900	0.67	0.88	0.37	0.718	1	-	-	-	-	-	-
Root Mean Square			1.32	1.45	0.76	0.910*							

* Obtained by (1) using these r.m.s. values.

based on the data digitized at the rate of one per second, as explained above. Overall root mean square values of these parameters and a resulting overall estimate of 0.910 for the correlation coefficient are also shown on Table VII.

In order to obtain a better insight in the range of the derived correlation coefficient estimates, the data for the 16 hours shown have been broken down further into intervals of five minutes, each containing 300 data points at the one-per-second sampling rate. Such a study is meaningful only when something is known about the serial correlation between successive readings. Serial correlation out to a lag of 300 seconds was determined for each hour. Fig. 23 shows typical results for four of the hours; Run 1 representing very high serial correlation out to a lag of 100 seconds, Run 9 suggesting an oscillatory trend, and Runs 12 and 14 showing a relatively fast drop of the serial correlation coefficient. Even without the use of rather involved significance tests, it may be seen that successive five-minute periods can be considered statistically independent, as the serial correlation coefficients drop to low values for a lag of 300 seconds in all cases.

Table VIII shows the resulting estimates of the cross-correlation coefficients between the two signals for all five-minute periods analyzed. Most of the values are above 0.9, only a few are below 0.5, and their range for each particular hour is well represented by the hourly values given on Table VII.

Finally, a possible dependence of the correlation coefficient estimates on other observed parameters was investigated. On Fig. 24, the estimates of the cross-correlation coefficient r are plotted versus the standard deviation s_x of one of the individual signals on the upper half (a), and versus the standard deviation s_{x-y} of the signal ratios on the lower half (b). All points represent the hourly

TABLE VIII

Correlation of Instantaneous Transmission Loss Values for Five-Minute Samples, 9250 and 9350 Mc/s

Time of Sample Within Hour	Run 1	2	3	4	5	6	7	8
00-05	.990	.906	.958	.892	.686	.827	.696	.713
05-10	.988	.930	.981	.925	.938	.789	.640	.714
10-15	.960	.791	.941	.936	.793	.791	.648	.786
15-20	.899	.794	.960	.933	.747	.789	.601	.667
20-25	.950	.957	.980	.503	.942	.848	.634	.439
25-30	.884	.986	.936	.799	.901	.795	.591	.713
30-35	.901	.988	.650	.845	.732	.787	.625	.371
35-40	.992	.955	.954	.746	.822	.775	.488	.704
40-45	.961	.985	.950	.976	.935	.837	.399	.708
45-50	.994	.923	.920	.882	.990	.689	.584	.595
50-55	.973	.950	.896	.967	.974	.729	.598	.671
55-60	.937	.979	.927	.687	.847	.707	.538	.731

	Run 9	12	13	14	15	16	17	18
00-05	.978	.859	.672	.834	.915	.919	.956	.778
05-10	.964	.912	.900	.735	.640	.752	.933	.344
10-15	.977	.908	.940	.716	.835	.693	.959	.757
15-20	.951	.912	.910	.742	.749	.868	.918	.787
20-25	.958	.872	.608	.677	.695	.580	.940	.728
25-30	.986	.843	.751	.517	.529	.717	.761	.739
30-35	.909	.941	.925	.740	.844	.535	.752	.948
35-40	.969	.861	.812	.867	.919	.866	.650	.949
40-45	.815	.839	.945	.674	.734	.626	.428	.898
45-50	.860	.842	.911	.698	.808	.855	.937	.843
50-55	.945	.920	.785	.780	.949	.967	.951	.863
55-60	.987	.832	.635	.755	.969	.901	.251	.846

data taken from Table VII. A convenient ordinate scale for the correlation coefficient was chosen arbitrarily. There is an apparent trend in the dependence of the correlation coefficient on the standard deviation of the individual signals, but no such trend appears in its dependence on the standard deviation of the signal ratios. If now, as mentioned first in the introduction, two separate propagation mechanisms ("deep-fading" and super-imposed scatter) are assumed, an analysis can be made of the effect of the mechanisms considered separately by assigning distinct variances and correlation coefficients to each mechanism. If each mechanism contributes to the overall variance and correlation, it should be possible to analyze the contribution of each separately. First the variance of the scatter component can be considered to be less than the total variance for any hour observed. This can be taken somewhat arbitrarily as 0.0625 db^2 from Fig. 24(a). Next the correlation coefficients of the two components are related in such a way that the trend in Fig. 24(a) can be removed by choosing an approximate value for the one pertaining to the scatter components. Although no direct estimates are available, a value of 0.5 removes the trend and is probably reasonable. With these assumptions the trend shown by the correlation coefficient assigned to the deep-fading component disappears; i.e., it becomes uniformly large regardless of the variability of the individual standard deviations. It is not possible to state at this time whether such an assumption is reasonable, as the design of this experiment requires the consideration of space diversity as well as frequency diversity effects. Measurements of the correlation of phase fluctuations over much shorter line-of-sight paths in this frequency range are available [Norton, et al, 1961]. It is indicated there that this correlation is quite high for spacings of the order of magnitude used here. An analysis of Norton, Vogler, Mansfield, and Short [1955] showed that for paths with a small "scatter" component superimposed on a larger "steady"

(or slowly-varying) signal the variance of the phase fluctuations is the same as the variance of amplitude fluctuations. Thus it is quite likely that the observed results are due to the frequency separation more than due to space diversity.

Fig. 25 compares the cumulative distributions of the standard deviations s_{x-y} of the signal ratios with the cumulative distributions of the standard deviations of the individual signals, s_x and s_y. The data represent all five-minute samples for the 16 hourly runs. The distributions are nearly parallel, and, according to (1), should be separated by $\sqrt{2(1-r)}$, where r is the overall estimate of the correlation coefficient from Table VII. Inspection of Fig. 25 shows that this is approximately true; the ratio of the ordinates at any percentage point is not too different from $\sqrt{2(1-0.910)} = 0.424$.

4. EVALUATION AND CONCLUSIONS

In this experiment, propagation studies were performed with continuous-wave signals transmitted over a 113 km within-the-horizon propagation path on frequencies of 1040.1, 9250, and 9350 Mc/s. The two X-band frequencies were selected at a 100 Mc/s spacing in order to study coherence over such wide bandwidths in the 9000 Mc/s frequency range. The transmissions on 1040.1 Mc/s provide a comparison of general propagation characteristics in the two frequency ranges as well as a general check on the experiment, as transmission loss measurements in this range had previously been performed over the same path.

Transmission loss variations analyzed in terms of the distributions of hourly medians showed somewhat different characteristics during the two recording periods. This is not considered to be particularly significant because of the relatively short periods of measurements; in general, the variations observed were in good agreement with predicted values.

Studies of short-term (within-the-hour) variation of the transmission loss showed that space-wave fadeouts exist in the 9000 Mc/s range. A comparison of the space-wave fadeouts at 9000 and at 1000 Mc/s showed them to be more numerous at the higher frequency although of shorter duration. Only for very deep fadeouts on the order of 20 db or more below the reference values do the fadeout durations in the two frequency ranges become comparable.

Diurnal characteristics of the observed fadeouts for both frequency ranges reflect the continental climate of the region where the measurements were made. From observations made in Colorado, fadeouts appear to be more prevalent during nighttime hours, and they are almost completely absent around noon and in the early afternoon hours. Because of the similarity in the diurnal characteristics over a wide frequency range it would be reasonable to estimate diurnal trends on 9000 Mc/s in other regions by extrapolating previously observed data on lower frequencies [Barsis and Johnson, 1961]. Although not enough data are available to establish a seasonal trend, a similar extrapolation from previously observed data on lower frequencies seems to be justified [Bean, 1954; Barsis and Johnson, 1961].

A study of fadeout durations at arbitrary transmission loss levels as well as at levels referenced to the overall median transmission loss for a five-day recording period shows that fadeouts exist for an appreciable percentage of the time, and have to be taken into account in the design of systems over paths of this type and within the frequency ranges considered.

The primary analysis made on the data obtained involved an investigation of the coherence over a 100 Mc/s bandwidth in the 9000 Mc/s frequency range. Two analytical approaches were pursued. Correlation bandwidth has been well defined previously, and it is

generally assumed that adequate coherence is maintained so long as the correlation coefficient between the variations in signals at the extreme ends of the bandpass is greater than 0.5. Over the 100 Mc/s frequency separation used in the experiment the correlation coefficient was found almost always to be much higher than 0.5.

A related but different method of analysis was used in which the instantaneous ratio of the two signals at the extreme ends of the bandpass is examined. Variations in this ratio give a measure of the selective fading and are not influenced by non-selective fading. This ratio was analyzed in terms of its distribution over one-hour periods. The most widely dispersed ratios observed during a one-hour period had a standard deviation estimated as 1.81 db. The average of the estimated standard deviations of the ratios within one-hour periods was 0.76 db. This again indicates adequate coherence across a 100 Mc/s modulation bandwidth. It is possible that if the standard deviations of the ratios exceed 3 db, serious problems in transmitting information would begin to arise.

The actual correlation or signal ratio bandwidths may be somewhat better than the experiments indicate inasmuch as the propagation paths used were not exactly identical. The two transmitting and two receiving antennas were located side by side with the centers separated by approximately thirty wavelengths. During the first run (in January) the paths were parallel, while during the second (in March) they were crossed. Thus some degree of diversity was certainly present and influenced the result, tending to reduce the correlation between the two signals and increase the dispersion in the ratios. Consequently the results present a somewhat worse estimate of the bandwidth capabilities than would be the case if all the signal components had been propagated along exactly the same path.

If a correlation coefficient of 0.5 or greater is taken as an indication of coherence over a finite frequency band, the results of these measurements show that such coherence is obtainable during most of the time under the conditions of the experiment. There are short periods, however, when coherence may not be maintained. Also, within-the-hour signal variations in the form of prolonged space-wave fadeouts are likely to occur, and have to be allowed for in the system design.

These conclusions are based on measurements using two discrete frequencies at the ends of the 100 Mc/s band studied. There is no simple method for extending the results of these studies to a modulated signal occupying a 100 Mc/s frequency band, and it therefore seems desirable that tests be made using modulated signals over a path of this type before actual system development. It would also be desirable to extend the basic studies reported here to other climatic areas and other times of the year.

5. ACKNOWLEDGEMENTS

The studies reported here were made possible through the support of the U. S. Army Signal Research and Development Laboratories, who also supplied the X-band equipment used in the tests. The measurements were performed by personnel of the Tropospheric Measurements Section, and the analysis done by personnel of the Propagation-Terrain Effects Section, both of the Radio Propagation Engineering Division of the Central Radio Propagation Laboratory. The digitizing of the magnetic tape data and related work was performed by personnel from the Data Reduction Instrumentation Section of the

same Laboratory. Drafting work was done by J. C. Harman and his group, and the manuscript was typed by Mrs. D. J. Hunt and Miss S. J. Bush.

The authors wish to thank Mr. K. A. Norton for his review and suggestions.

6. REFERENCES

Barsis, A. P., J. W. Herbstreit, and K. O. Hornberg, Cheyenne Mountain tropospheric propagation experiments, NBS Circular 554 (Jan. 1955).

Barsis, A. P., and M. E. Johnson, Prolonged space-wave fadeouts in tropospheric propagation, NBS Technical Note 88, PB 161589 (Feb. 1961), $2.00.*

Bean, B. R., Prolonged space-wave fadeouts at 1046 Mc observed in Cheyenne Mountain propagation program, Proc. IRE 42, No. 5, 848-853 (May 1954).

Bean, B. R., and J. D. Horn, Radio-refractive-index climate near the ground, J. Research NBS 63D (Radio Prop.), No. 3, 259-271 (Nov.-Dec. 1959).

Bennett, C. A., and N. L. Franklin, Statistical analysis in chemistry and the chemical industry (John Wiley and Sons, Inc., New York, N. Y., 1954).

Janes, H. B., and P. I. Wells, Some tropospheric scatter propagation measurements near the radio horizon, Proc. IRE 43, No. 10, 1336-1340 (Oct. 1955).

Norton, K. A., Transmission loss in radio propagation, Proc. IRE 41, No. 1, 146-152 (Jan. 1953).

Norton, K. A., System loss in radio-wave propagation, Proc. IRE 47, No. 9, 1661-1662 (Sept. 1959).

Norton, K. A., P. L. Rice, and L. E. Vogler, The use of the angular distance in estimating transmission loss and fading range for propagation through a turbulent atmosphere over irregular terrain, Proc. IRE 43, No. 10, 1488-1526 (Oct. 1955).

Norton, K. A., L. E. Vogler, W. V. Mansfield, and P. J. Short, The probability distribution of the amplitude of a constant vector plus a Rayleigh-distributed vector, Proc. IRE 43, No. 10, 1354-1361 (Oct. 1955).

---

* Order by PB number from the Office of Technical Services, U. S. Department of Commerce, Washington 25, D. C. Foreign remittances must be in U. S. exchange and must include one-fourth of the publication price to cover mailing costs.

Norton, K. A., J. W. Herbstreit, H. B. Janes, K. O. Hornberg, C. F. Peterson, A. F. Barghausen, W. E. Johnson, P. I. Wells, M. C. Thompson, Jr., M. J. Vetter, and A. W. Kirkpatrick, An experimental study of phase variations in line-of-sight microwave transmission, NBS Monograph 33 (1961).

Rice, P. L., A. G. Longley, and K. A. Norton, Prediction of the cumulative distribution of ground wave and tropospheric wave transmission loss, NBS Technical Note 15, PB 151374 (July 1959), $1.50.*

* Order by PB number from the Office of Technical Services, U. S. Department of Commerce, Washington 25, D. C. Foreign remittances must be in U. S. exchange and must include one-fourth of the publication price to cover mailing costs.

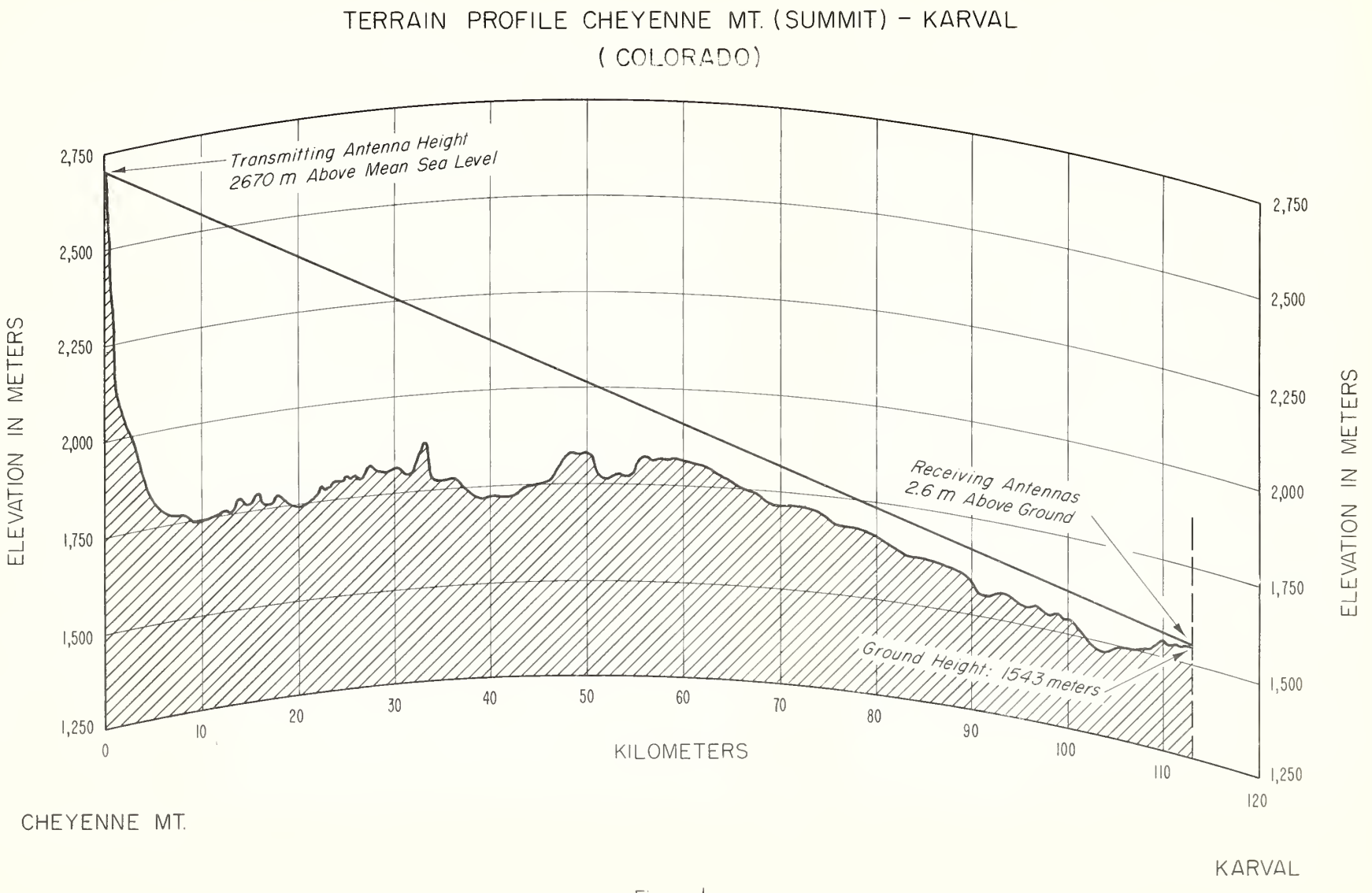
TERRAIN PROFILE CHEYENNE MT. (SUMMIT) – KARVAL
(COLORADO)
Transmitting Antenna Height
2670 m Above Mean Sea Level
Receiving Antennas
2.6 m Above Ground
Ground Height: 1543 meters
ELEVATION IN METERS
2,750
2,500
2,250
2,000
1,750
1,500
1,250
0
10
20
30
40
50
60
70
80
90
100
110
120
KILOMETERS
CHEYENNE MT.
KARVAL

Figure 1

ANTENNA ARRANGEMENT

ANTENNA FOREGROUND

CHEYENNE MOUNTAIN TRANSMITTER LOCATION

Figure 2

COMPLETE RECEIVING INSTALLATION

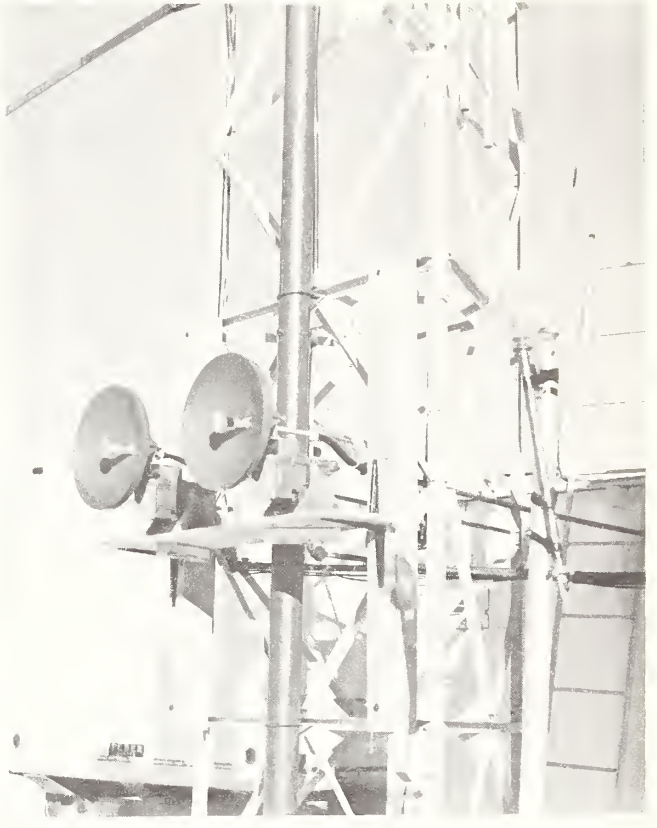

9250 AND 9350 Mc/s ANTENNAS

KARVAL RECEIVING LOCATION

Figure 3

CALCULATED DEPENDENCE OF BASIC TRANSMISSION LOSS ON RECEIVING ANTENNA HEIGHT FOR CHEYENNE MOUNTAIN – KARVAL PATH

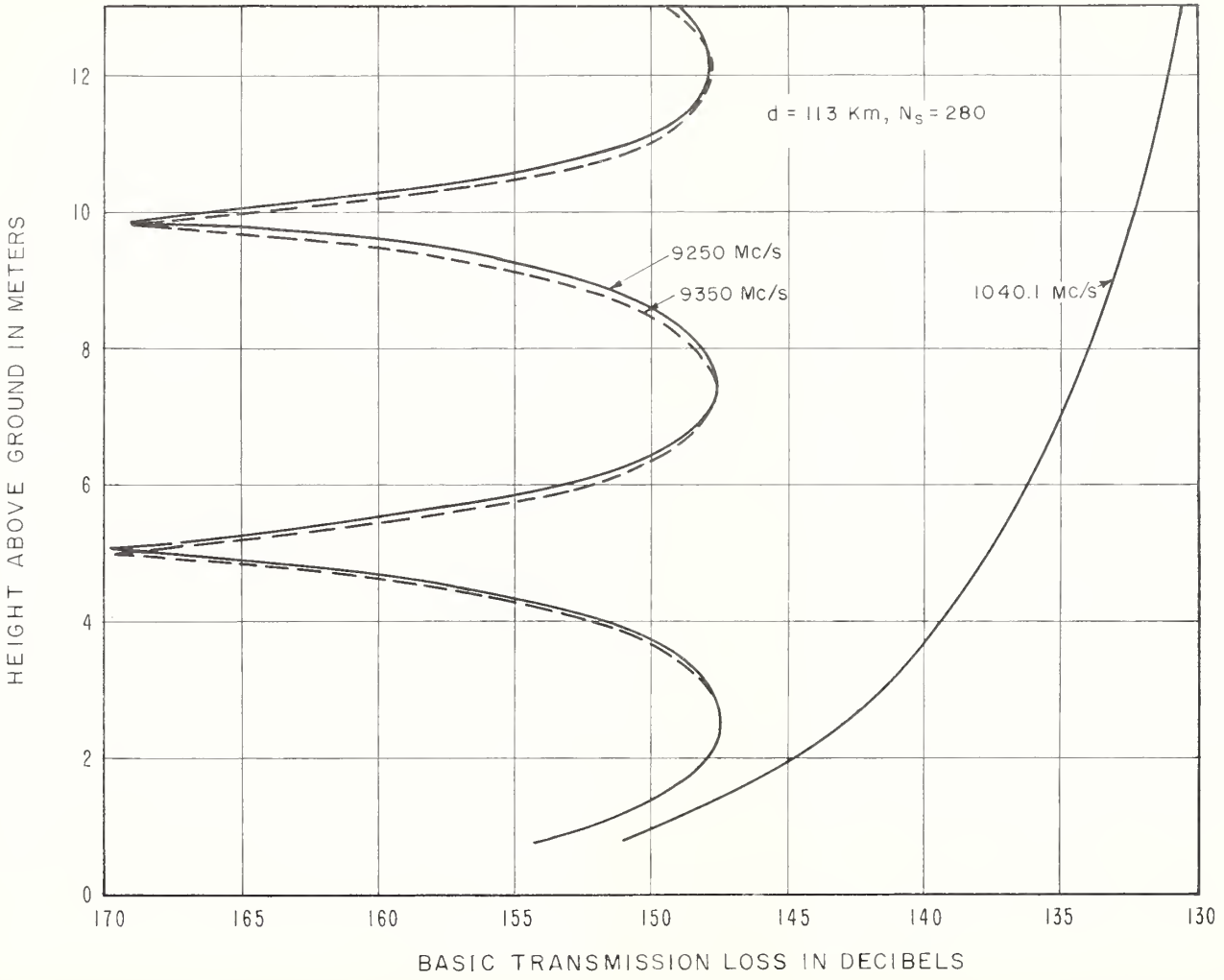

Figure 4

CUMULATIVE DISTRIBUTIONS OF HOURLY BASIC TRANSMISSION LOSS MEDIANS
FOR CHEYENNE MOUNTAIN- KARVAL PATH, 1040.1 Mc/s

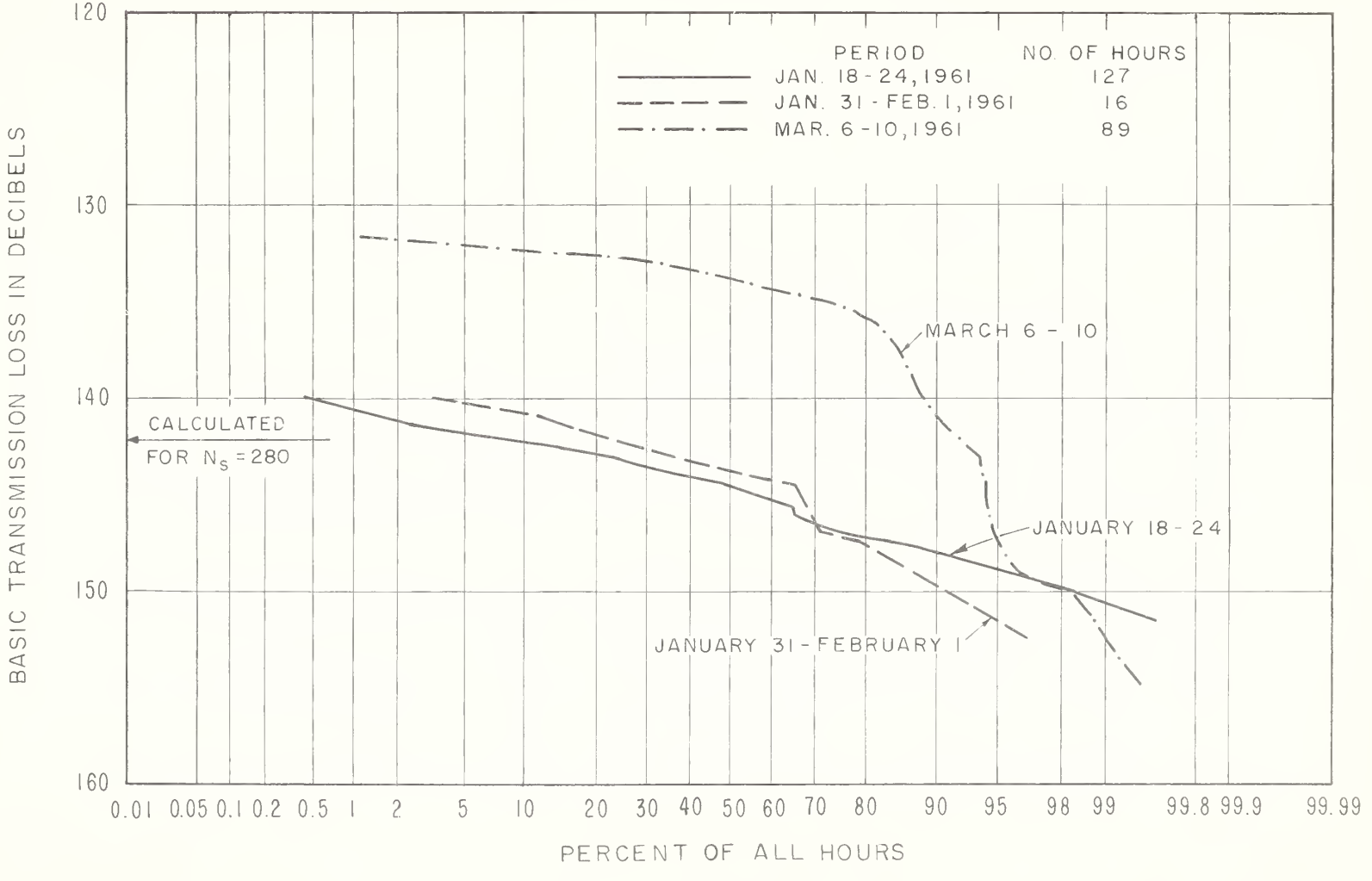

Figure 5

CUMULATIVE DISTRIBUTIONS OF HOURLY BASIC TRANSMISSION LOSS MEDIANS FOR CHEYENNE MOUNTAIN - KARVAL PATH, 9250 AND 9350 Mc/s

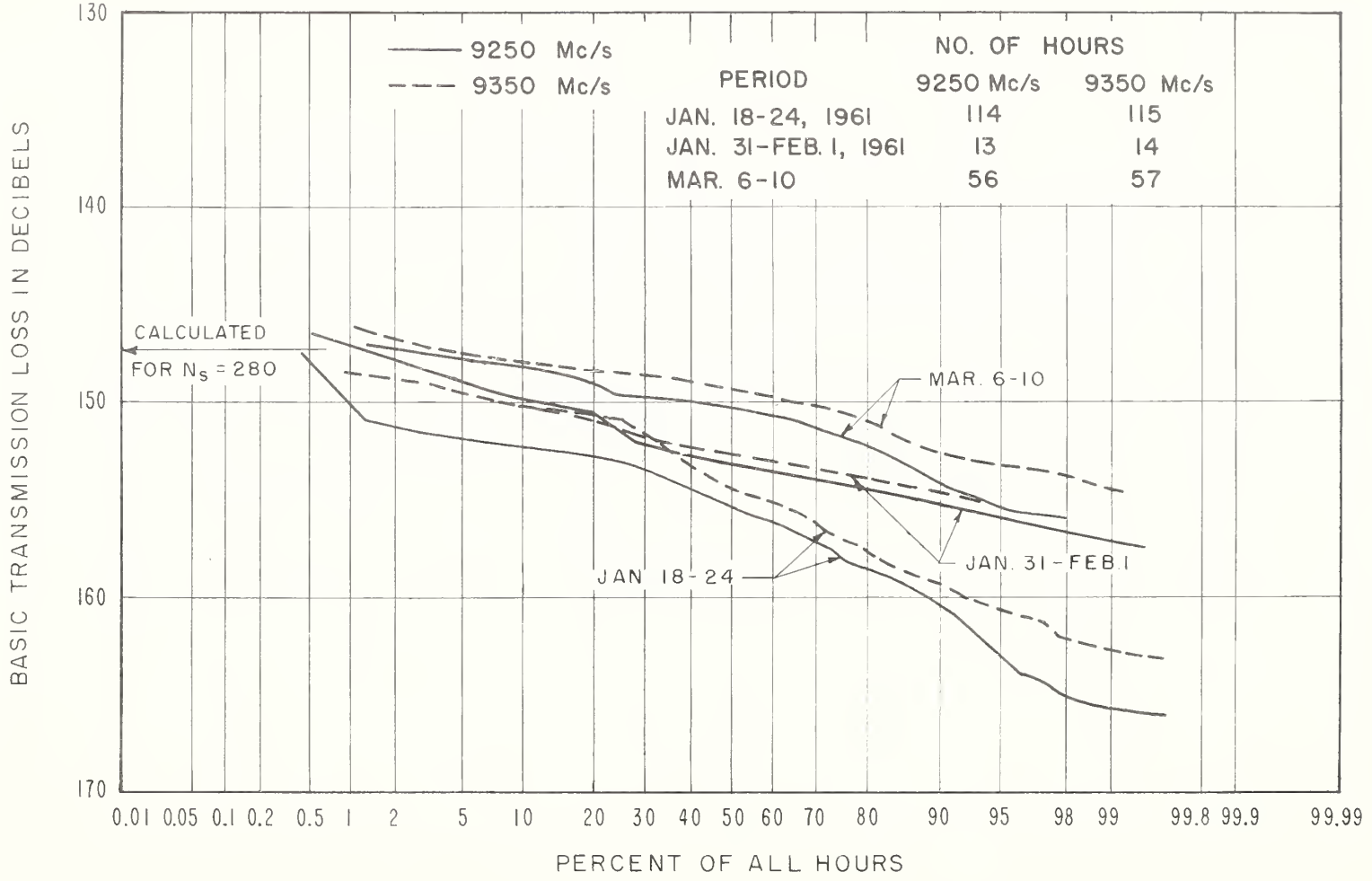

Figure 6

RECORDING CHART SAMPLES FOR CHEYENNE MOUNTAIN-KARVAL PATH

1600 – 1630, MARCH 9, 1961 (NO SPACE-WAVE FADEOUTS)

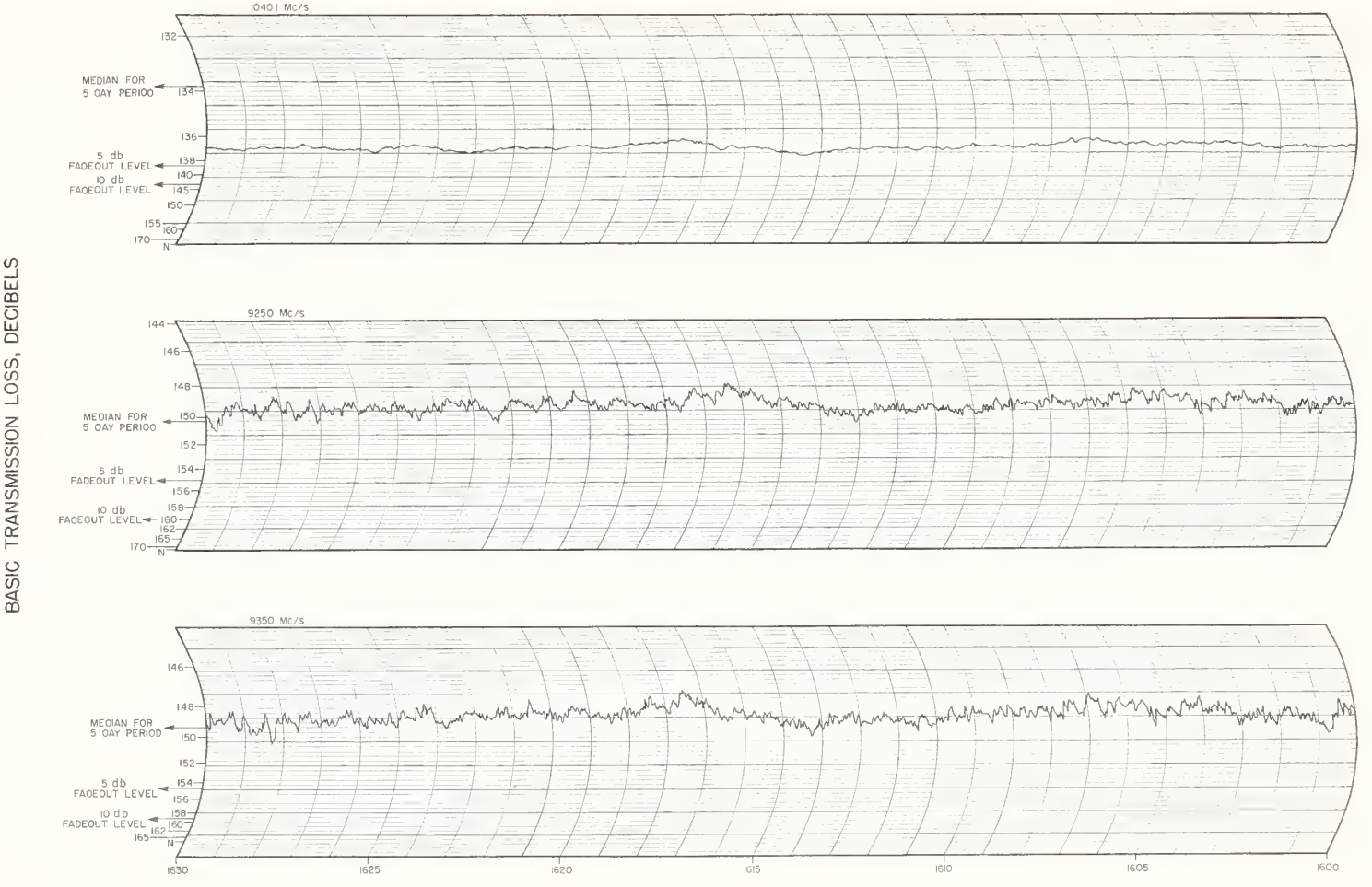

Figure 7

RECORDING CHART SAMPLES FOR CHEYENNE MOUNTAIN-KARVAL PATH

2230 - 2300, MARCH 6, 1961 (SPACE-WAVE FADEOUTS PRESENT)

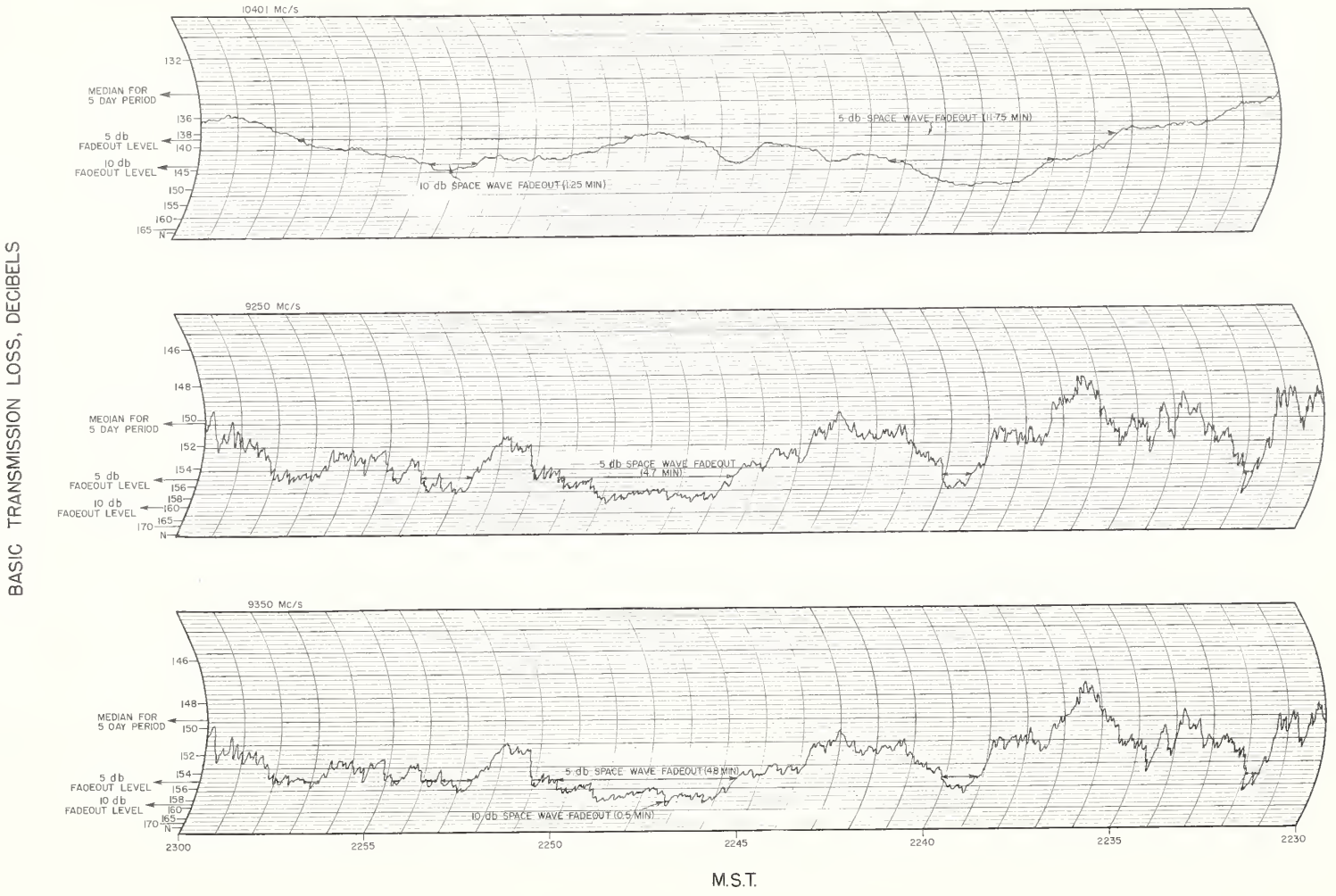

Figure 8

DIURNAL VARIATION OF FADEOUT CHARACTERISTICS

CHEYENNE MOUNTAIN – KARVAL PATH

WINTER 1961

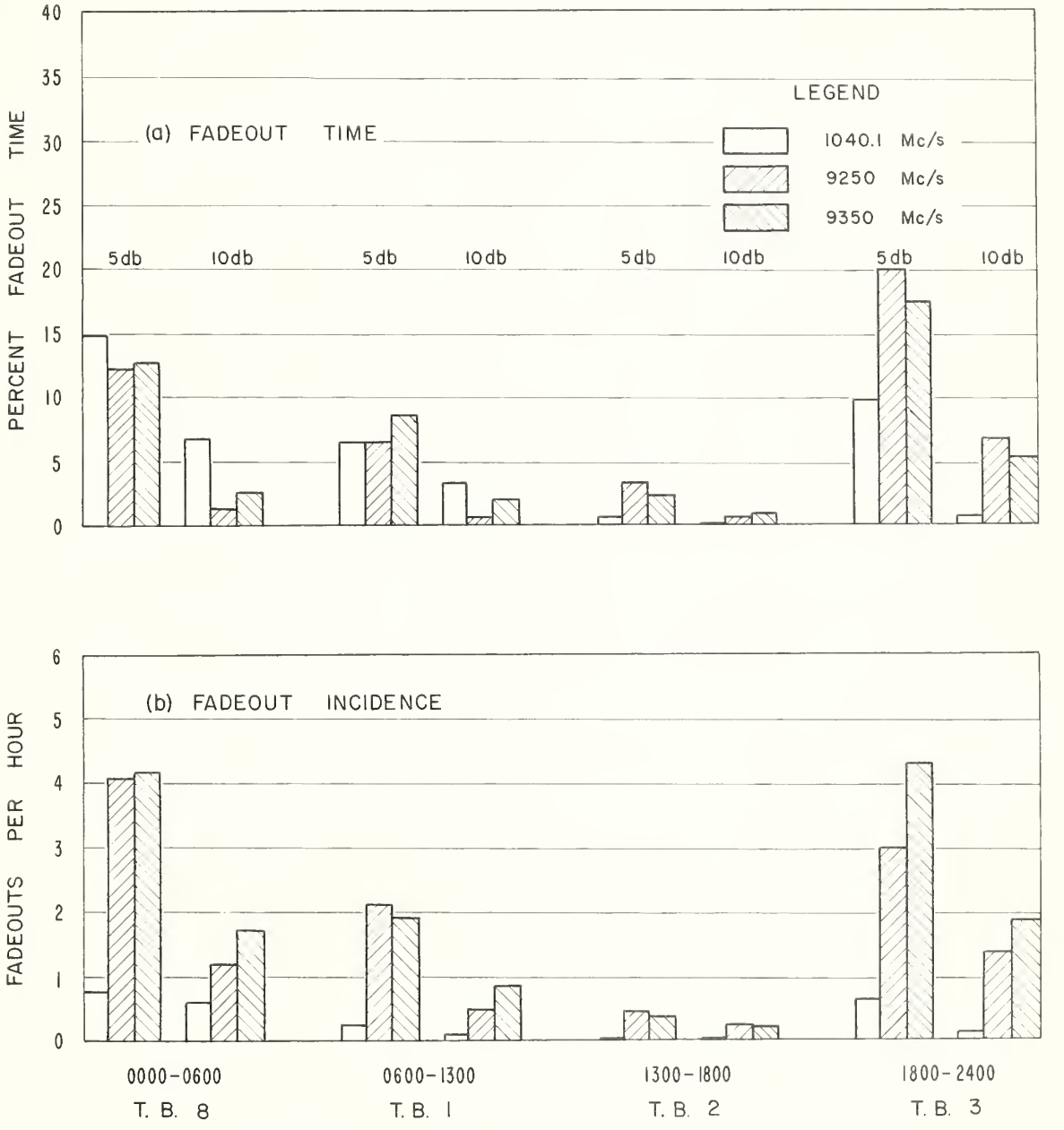

Figure 9

CHEYENNE MOUNTAIN - KARVAL PATH
DISTRIBUTION OF FADEOUT DURATIONS AT VARIOUS LEVELS
BELOW THE REFERENCE VALUE (5 DAY MEDIAN)
JANUARY and MARCH, 1961

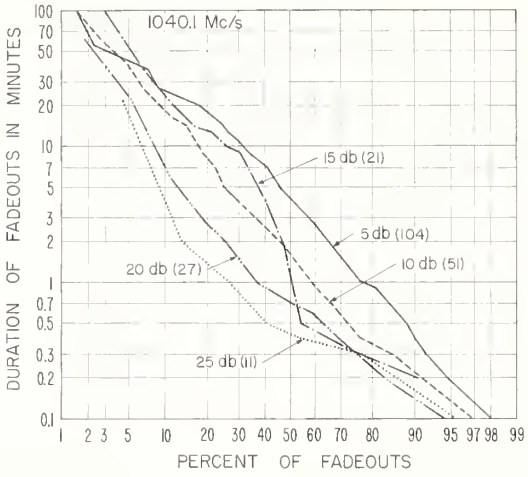

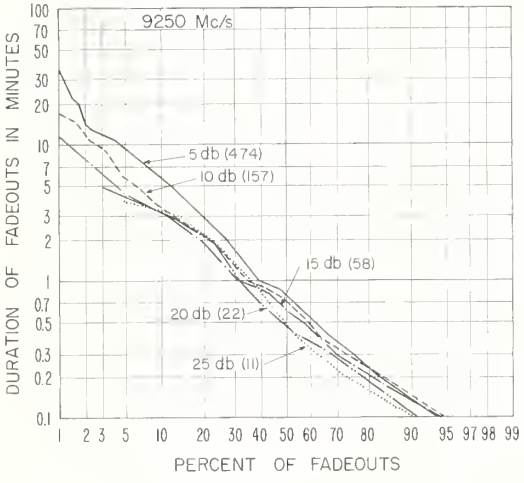

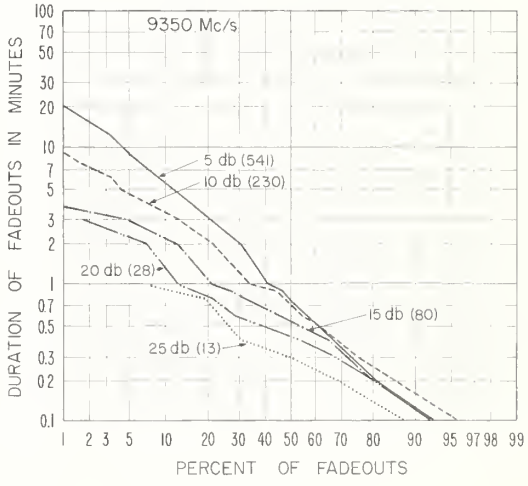

FIGURE 10

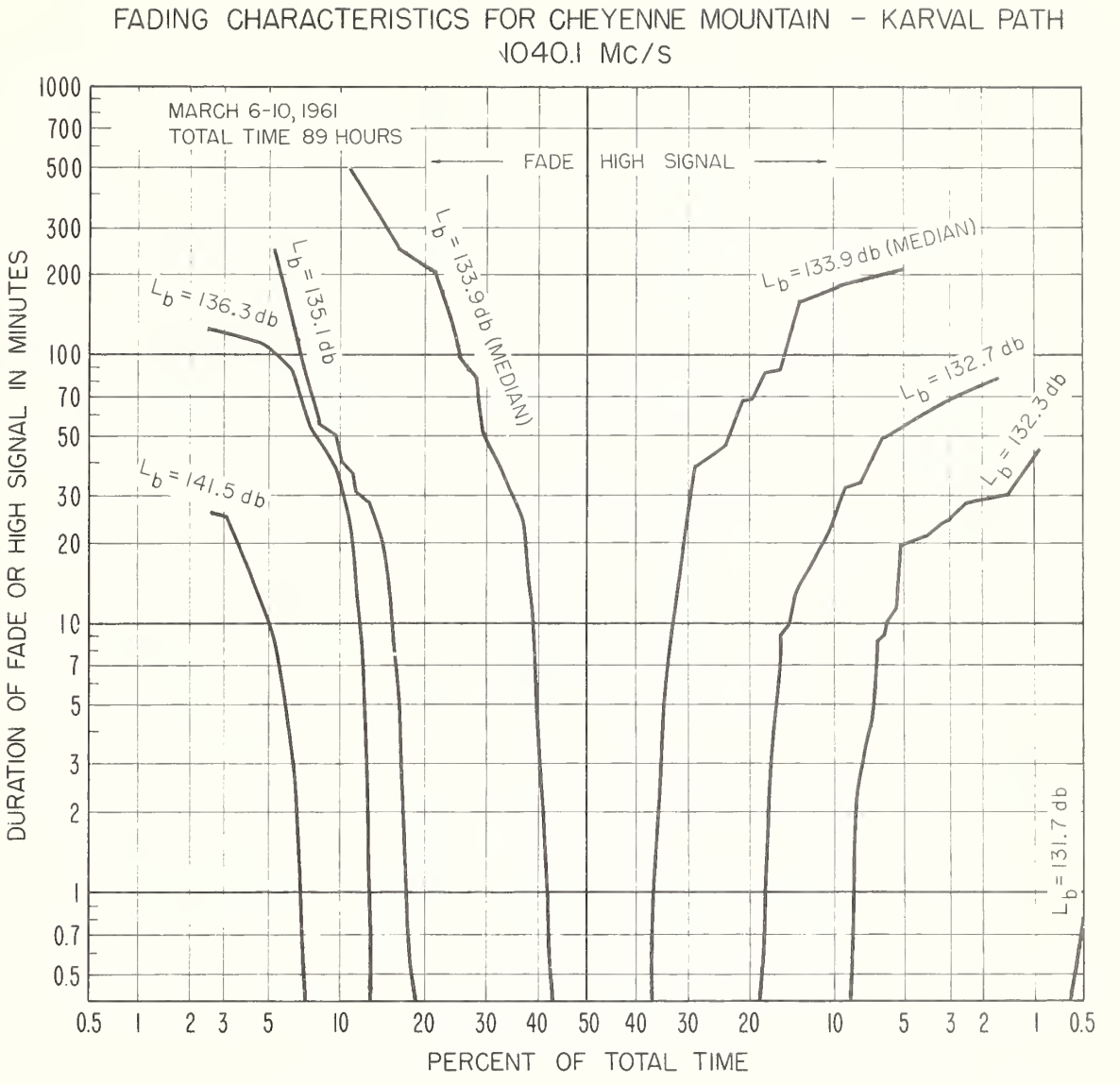
FADING CHARACTERISTICS FOR CHEYENNE MOUNTAIN - KARVAL PATH
1040.1 Mc/s
MARCH 6-10, 1961
TOTAL TIME 89 HOURS
FADE
HIGH SIGNAL
L_b = 136.3 db
L_b = 135.1 db
L_b = 133.9 db (MEDIAN)
L_b = 141.5 db
L_b = 133.9 db (MEDIAN)
L_b = 132.7 db
L_b = 132.3 db
L_b = 131.7 db
DURATION OF FADE OR HIGH SIGNAL IN MINUTES
1000
700
500
300
200
100
70
50
30
20
10
7
5
3
2
1
0.7
0.5
0.5 1 2 3 5 10 20 30 40 50 40 30 20 10 5 3 2 1 0.5
PERCENT OF TOTAL TIME

Figure 11

FADING CHARACTERISTICS FOR CHEYENNE MOUNTAIN - KARVAL PATH
9250 Mc/s

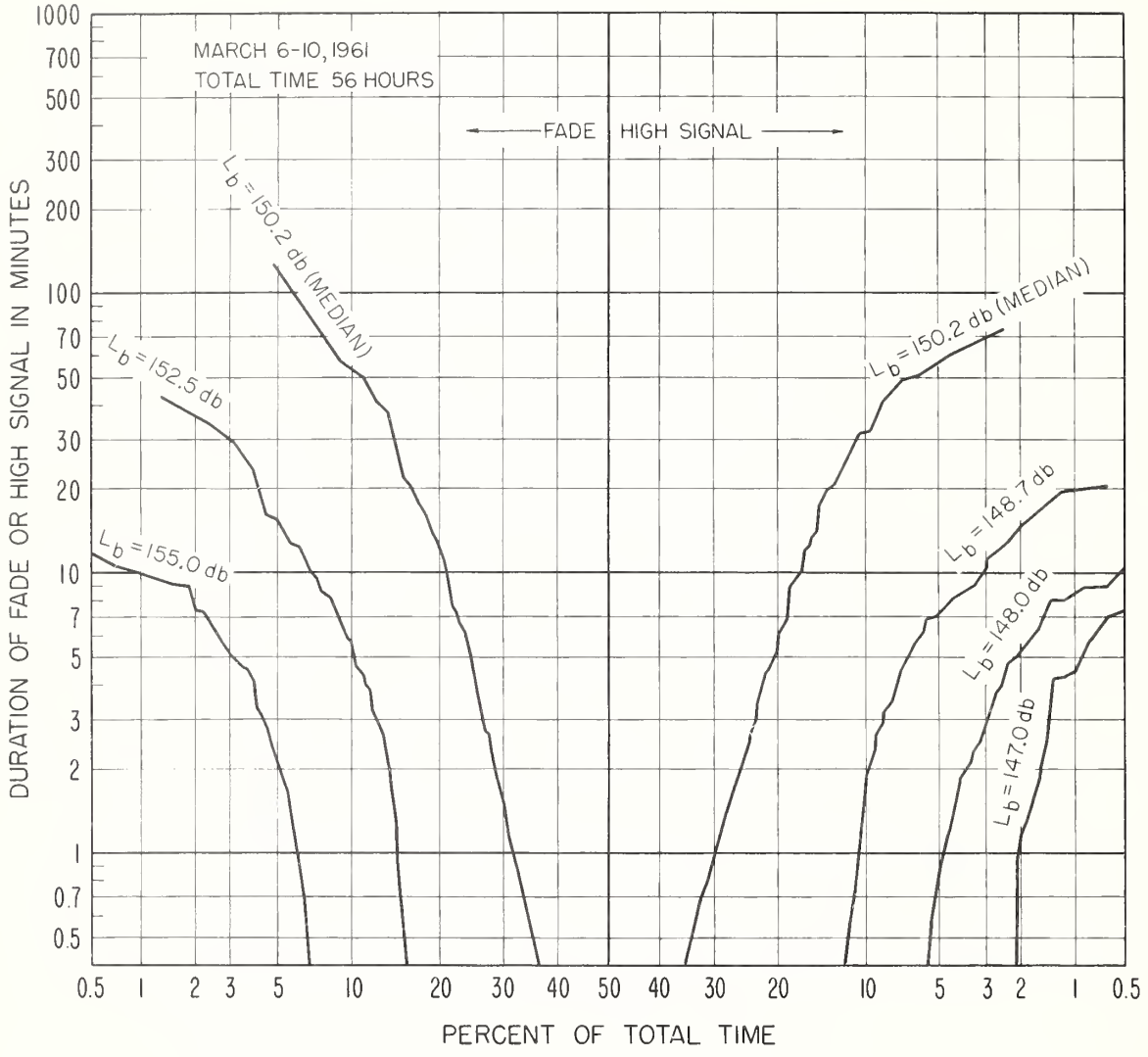

Figure 12

FADING CHARACTERISTICS FOR CHEYENNE MOUNTAIN – KARVAL PATH
9350 Mc/s

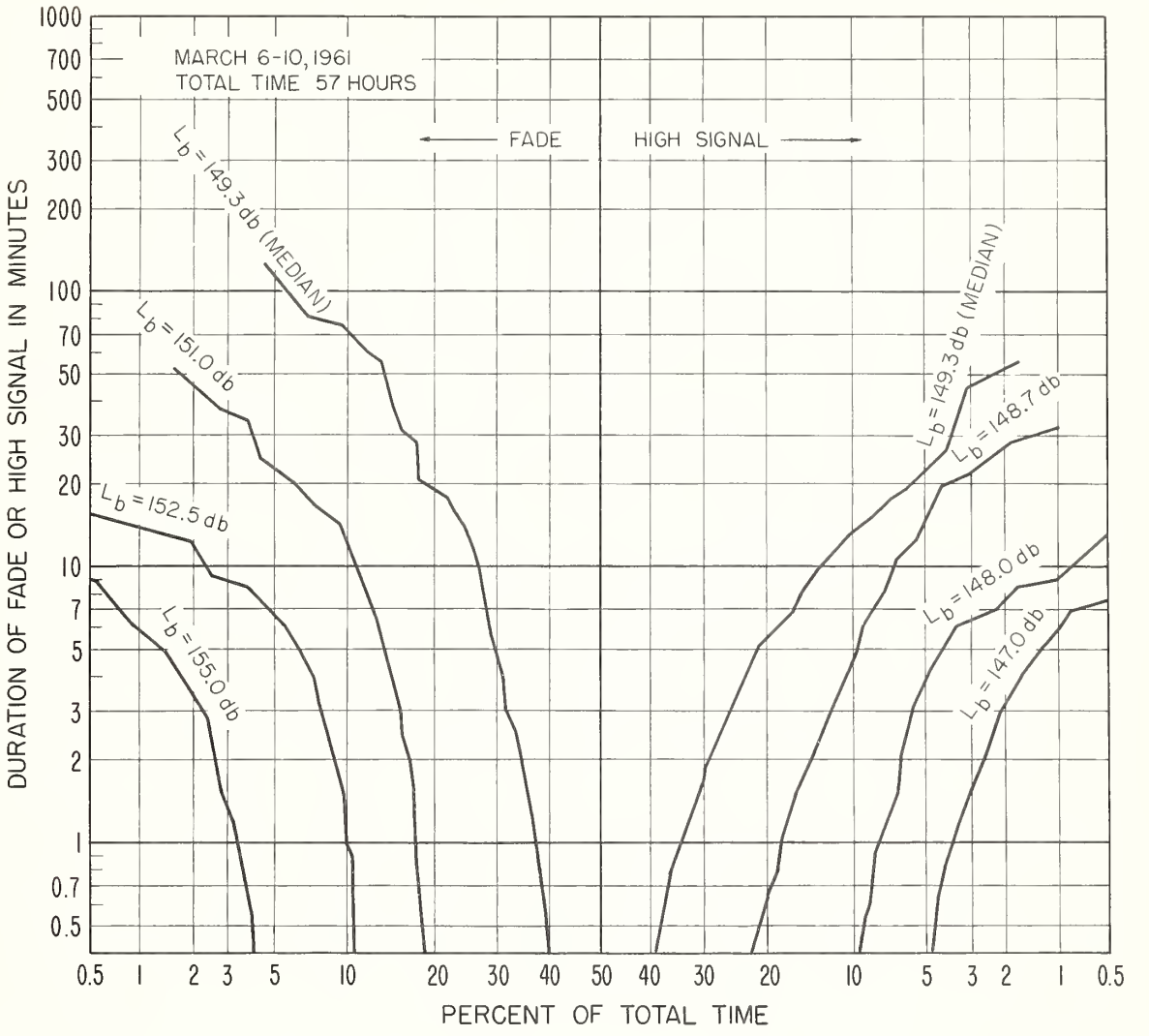

Figure 13

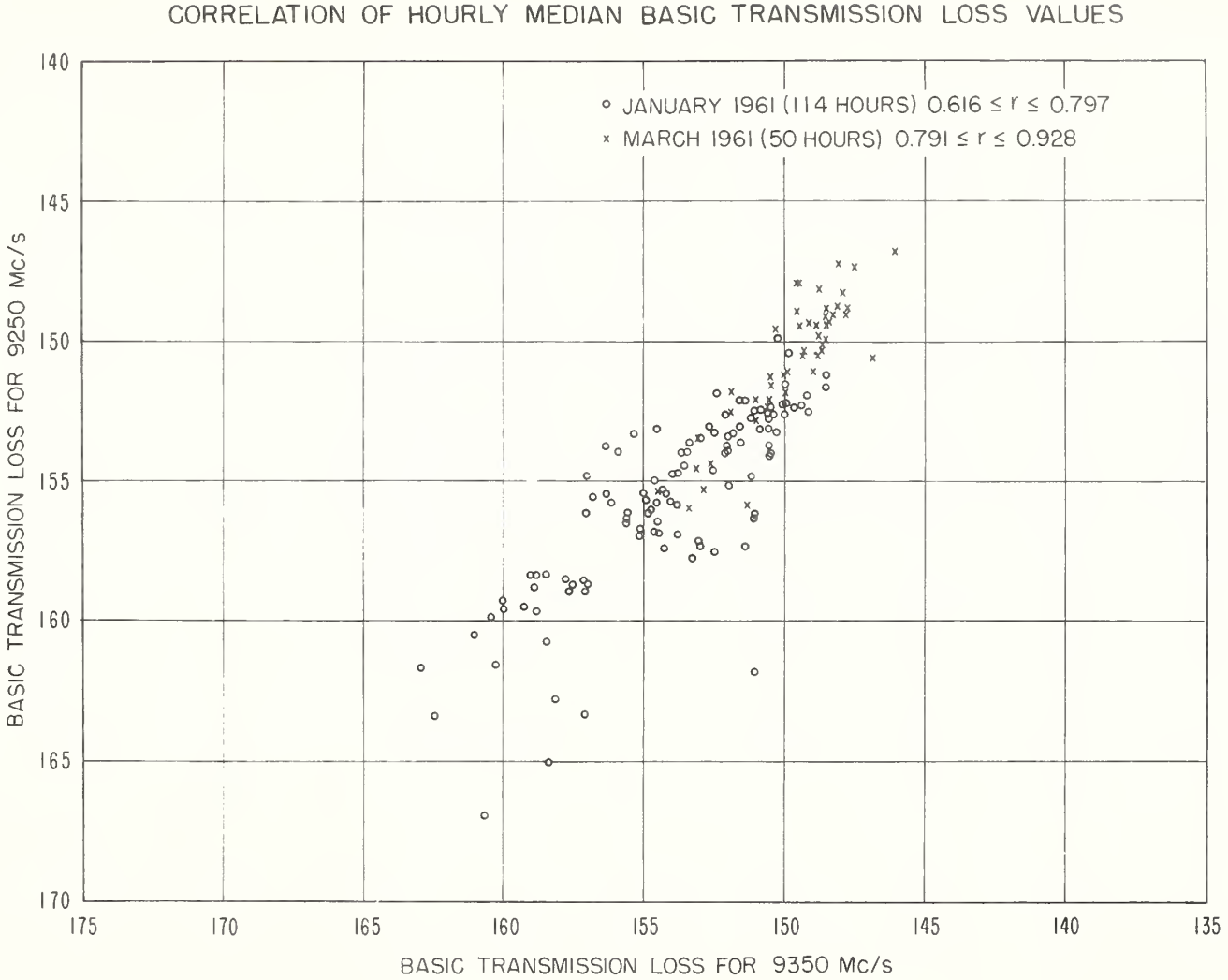
CORRELATION OF HOURLY MEDIAN BASIC TRANSMISSION LOSS VALUES
o JANUARY 1961 (114 HOURS) 0.616 ≤ r ≤ 0.797
× MARCH 1961 (50 HOURS) 0.791 ≤ r ≤ 0.928
BASIC TRANSMISSION LOSS FOR 9250 Mc/s
140
145
150
155
160
165
170
175
170
165
160
155
150
145
140
135
BASIC TRANSMISSION LOSS FOR 9350 Mc/s

Figure 14

CHEYENNE MOUNTAIN - KARVAL PATH
DECIBEL DIFFERENCE OF INSTANTANEOUS
TRANSMISSION LOSS VALUES ON 9250 AND 9350 Mc/s

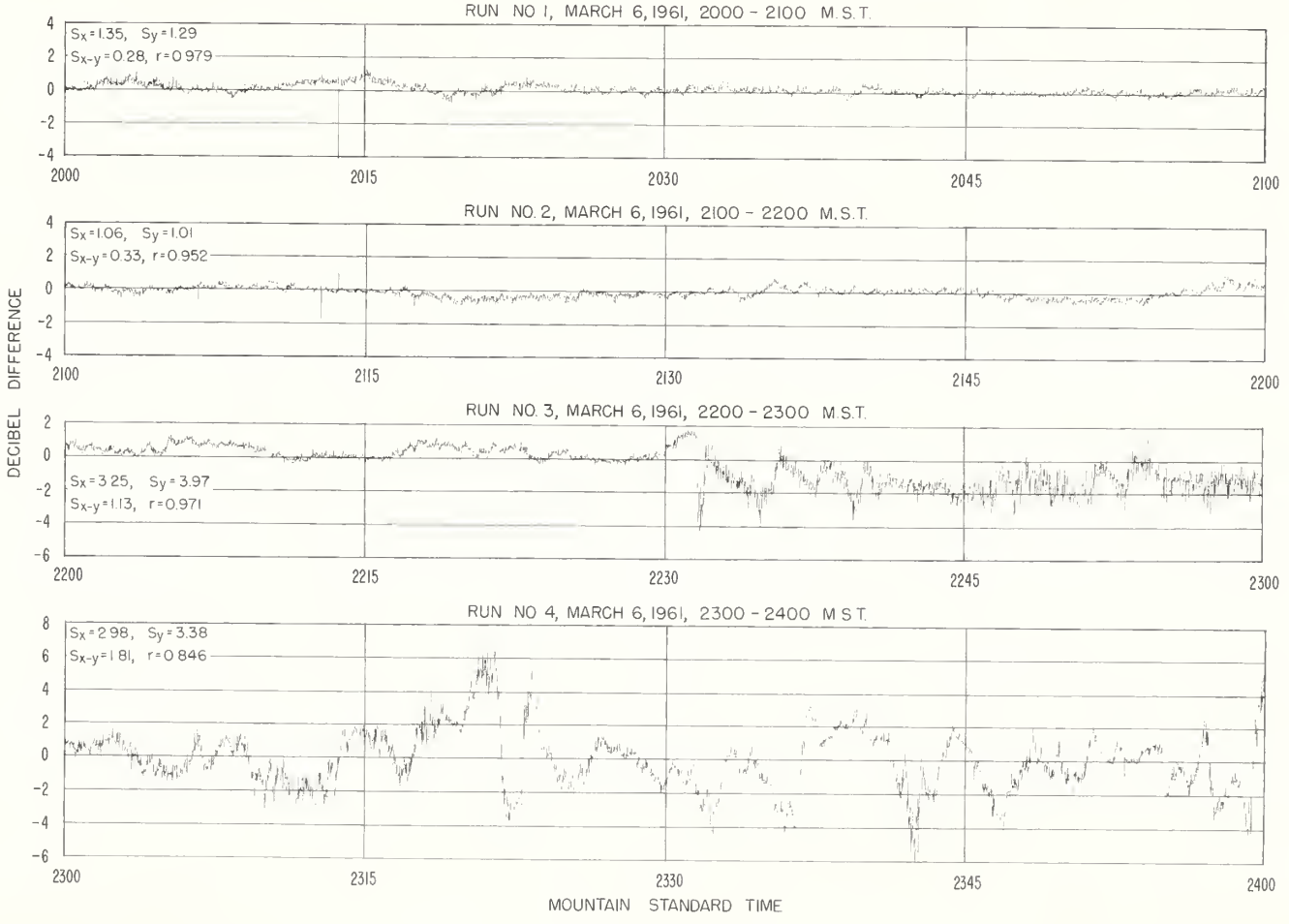

Figure 15

CHEYENNE MOUNTAIN - KARVAL PATH
DECIBEL DIFFERENCE OF INSTANTANEOUS
TRANSMISSION LOSS VALUES ON 9250 AND 9350 MC/S

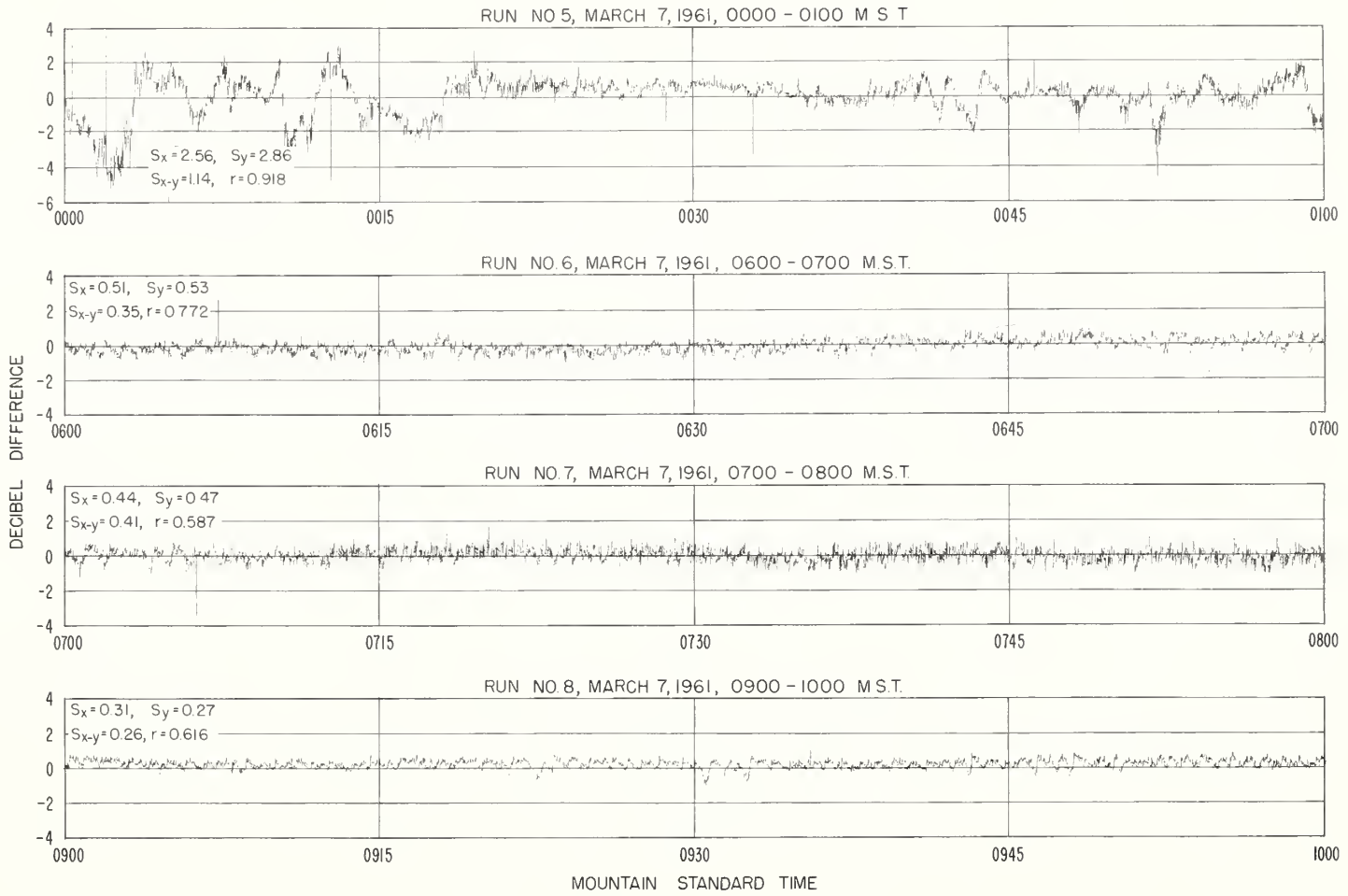

Figure 16

CHEYENNE MOUNTAIN - KARVAL PATH
DECIBEL DIFFERENCE OF INSTANTANEOUS
TRANSMISSION LOSS VALUES ON 9250 AND 9350 Mc/s

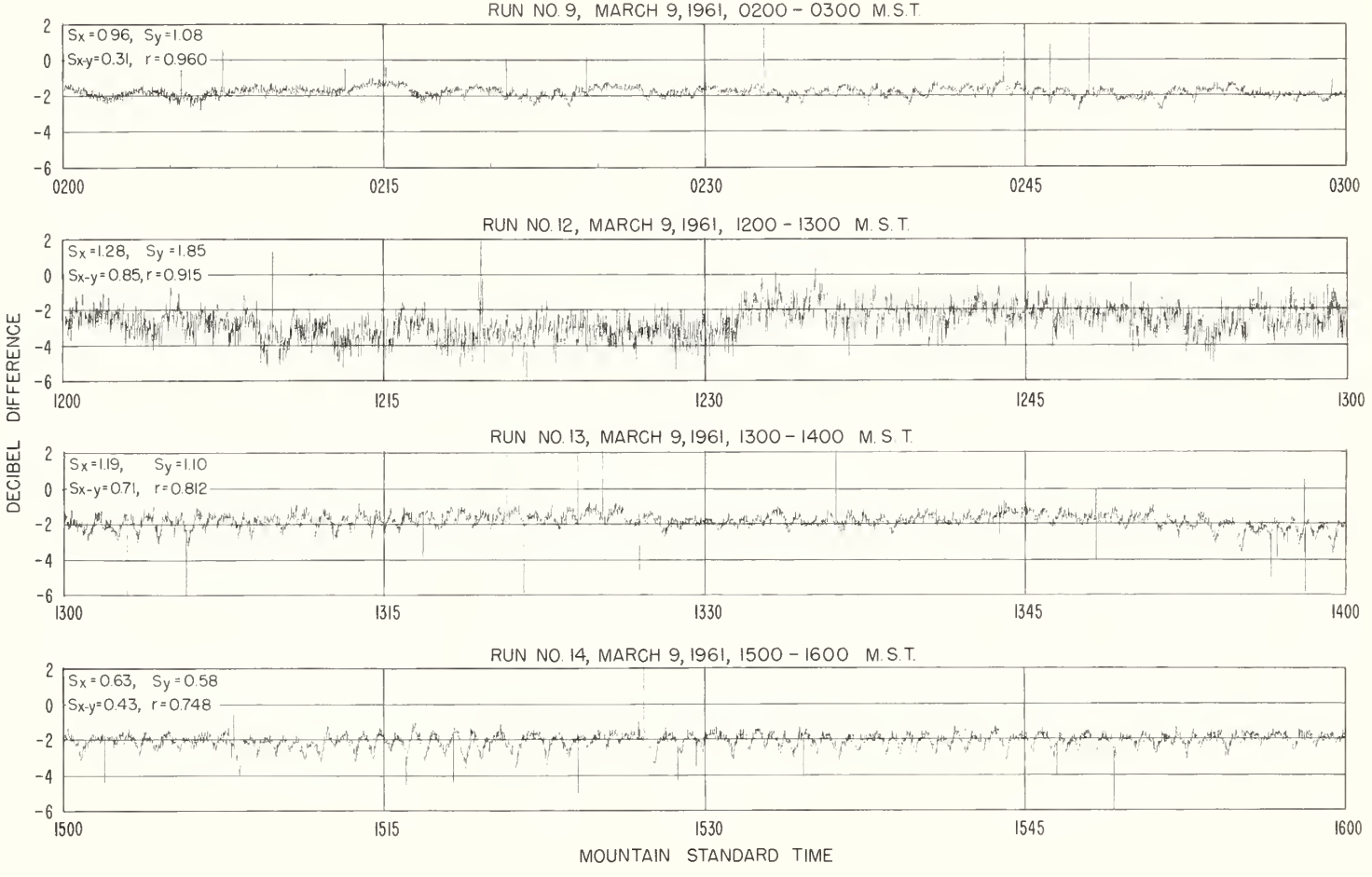

Figure 17

CHEYENNE MOUNTAIN - KARVAL PATH
DECIBEL DIFFERENCE OF INSTANTANEOUS
TRANSMISSION LOSS VALUES ON 9250 AND 9350 MC/S

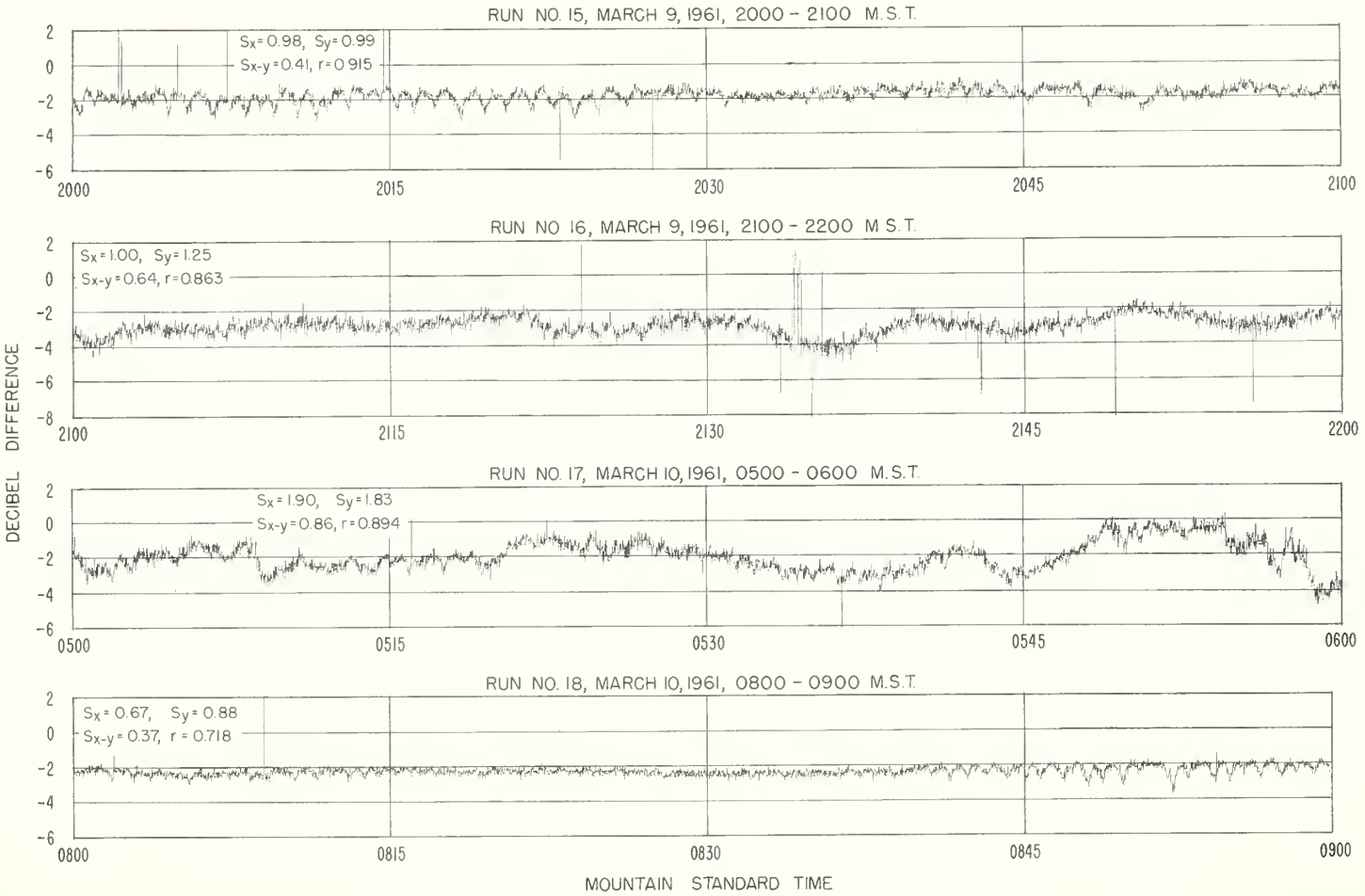

Figure 18

CHEYENNE MOUNTAIN - KARVAL PATH
CORRELATION DIAGRAM OF SIMULTANEOUSLY OBSERVED INSTANTANEOUS
TRANSMISSION LOSS VALUES ON 9250 AND 9350 Mc/s

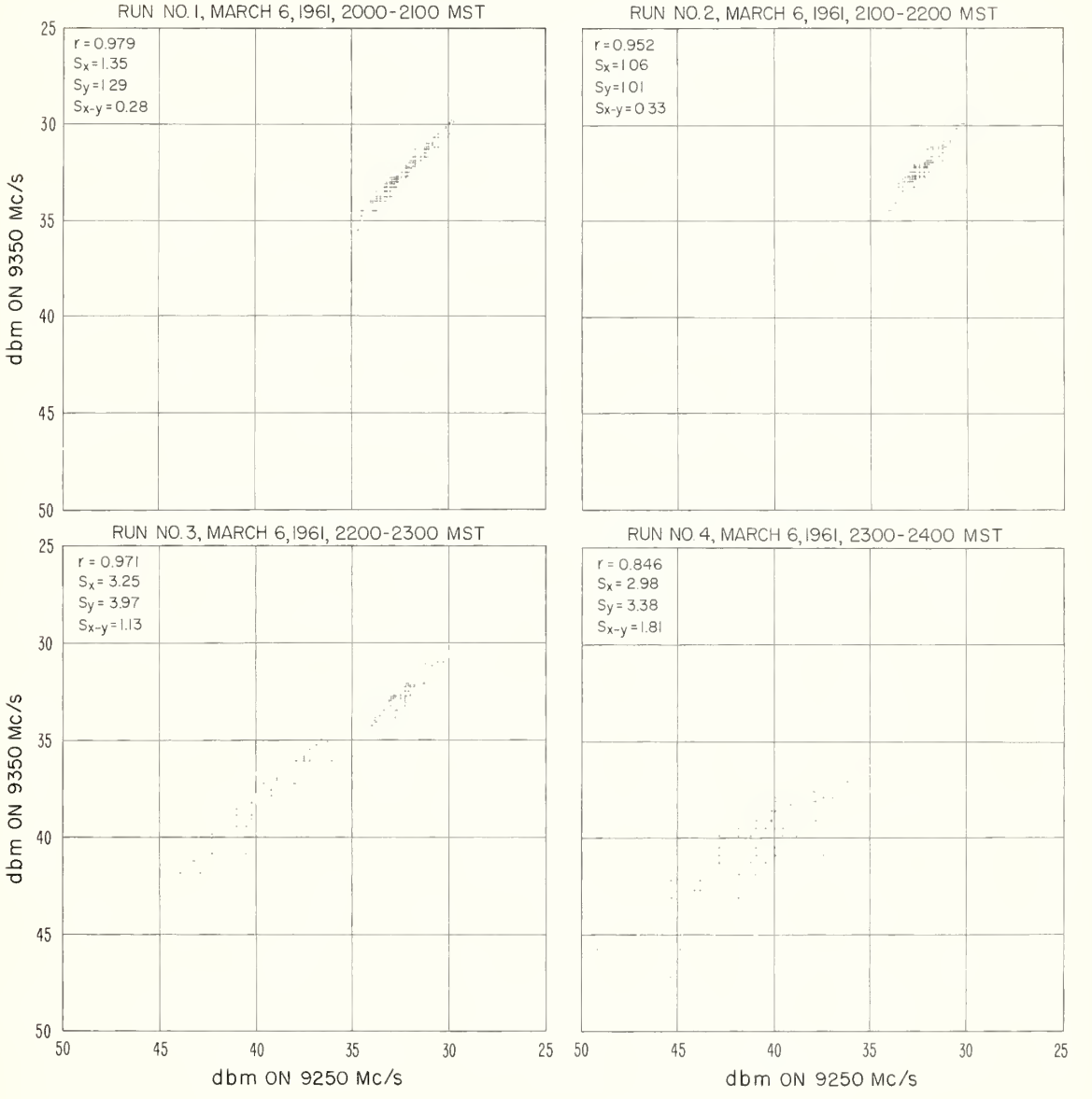

Figure 19

CHEYENNE MOUNTAIN - KARVAL PATH
CORRELATION DIAGRAM OF SIMULTANEOUSLY OBSERVED INSTANTANEOUS
TRANSMISSION LOSS VALUES ON 9250 AND 9350 Mc/s

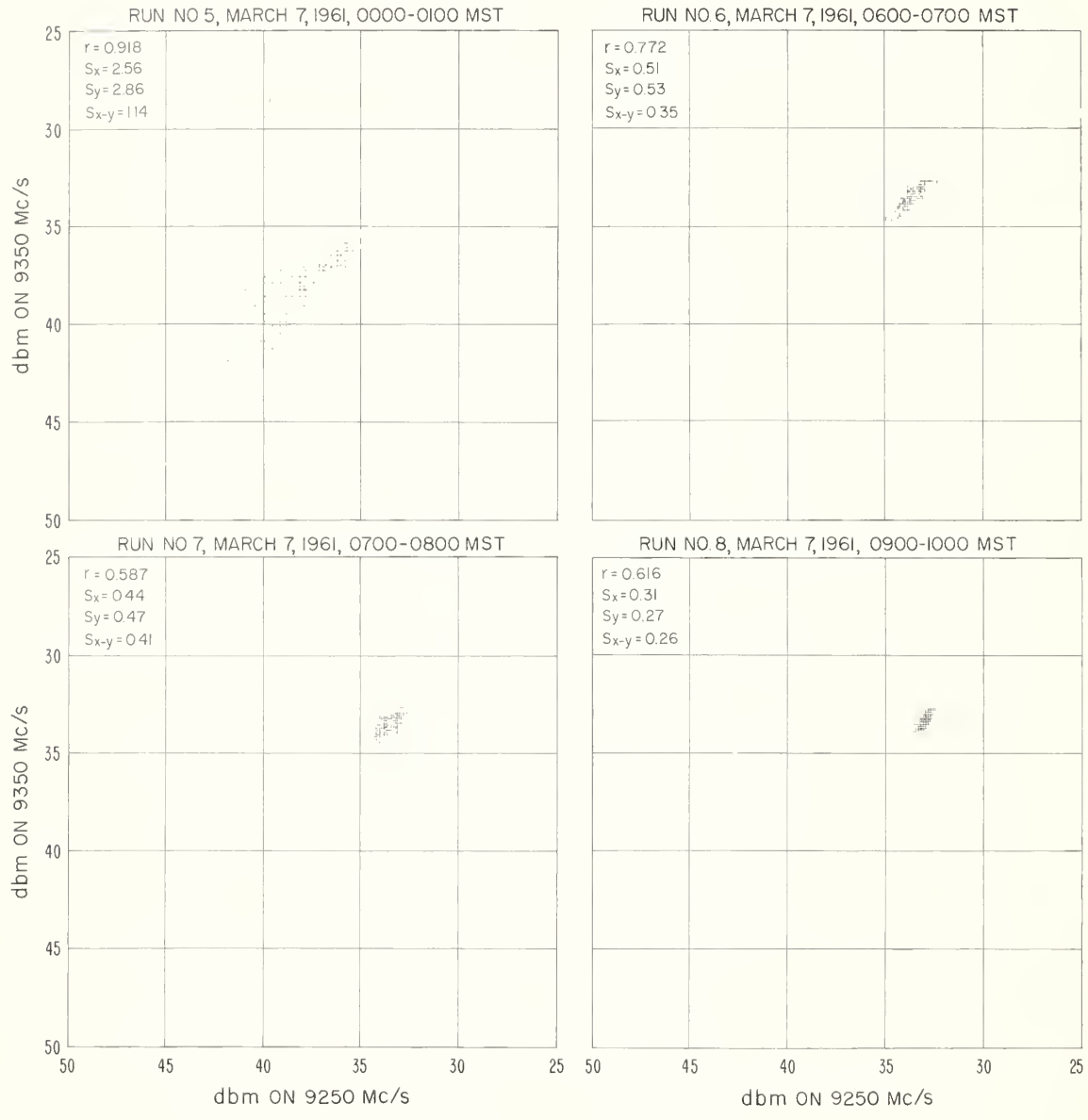

Figure 20

CHEYENNE MOUNTAIN - KARVAL PATH
CORRELATION DIAGRAM OF SIMULTANEOUSLY OBSERVED INSTANTANEOUS
TRANSMISSION LOSS VALUES ON 9250 AND 9350 Mc/s

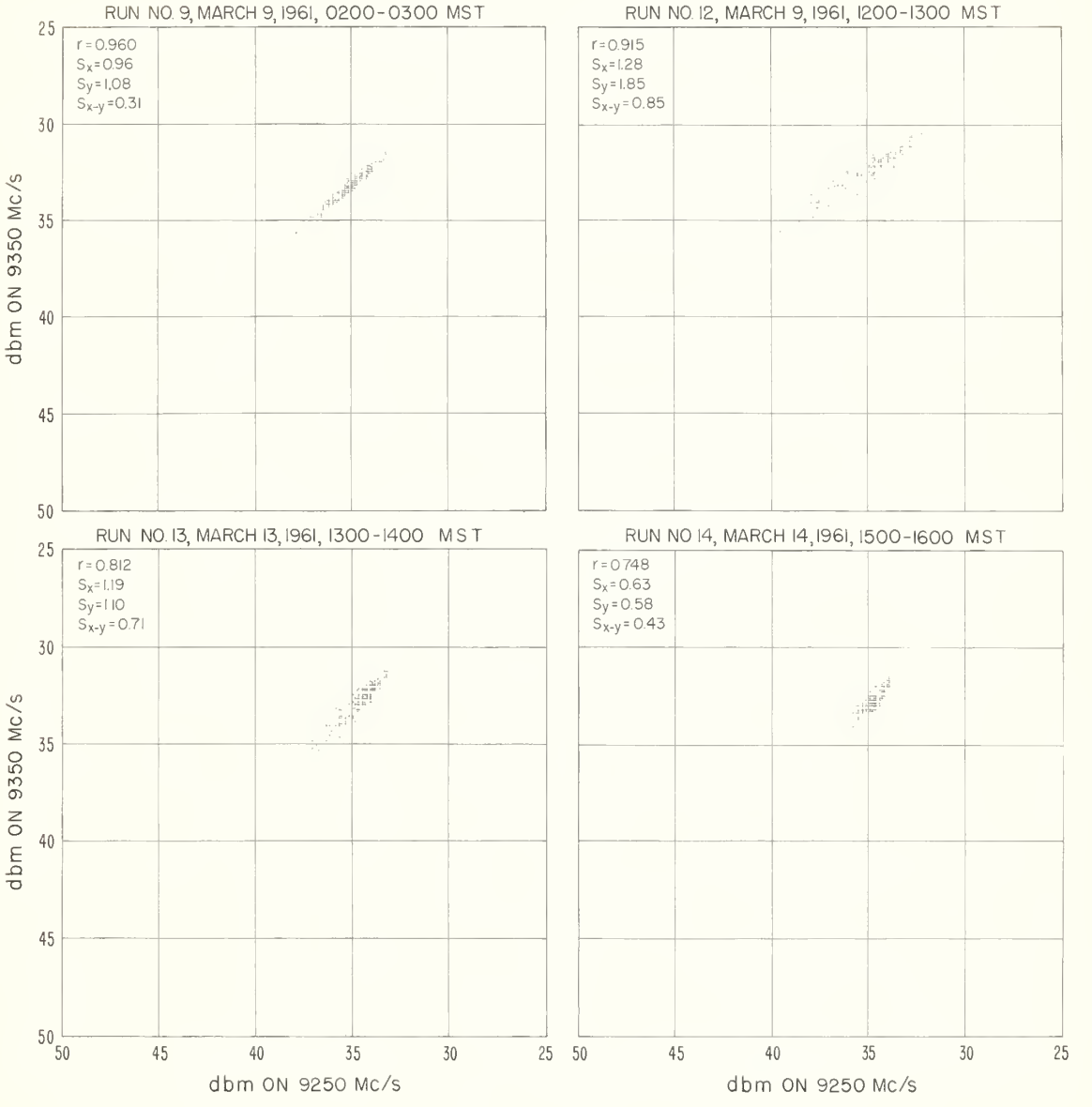

Figure 21

CHEYENNE MOUNTAIN - KARVAL PATH
CORRELATION DIAGRAM OF SIMULTANEOUSLY OBSERVED INSTANTANEOUS
TRANSMISSION LOSS VALUES ON 9250 AND 9350 Mc/s

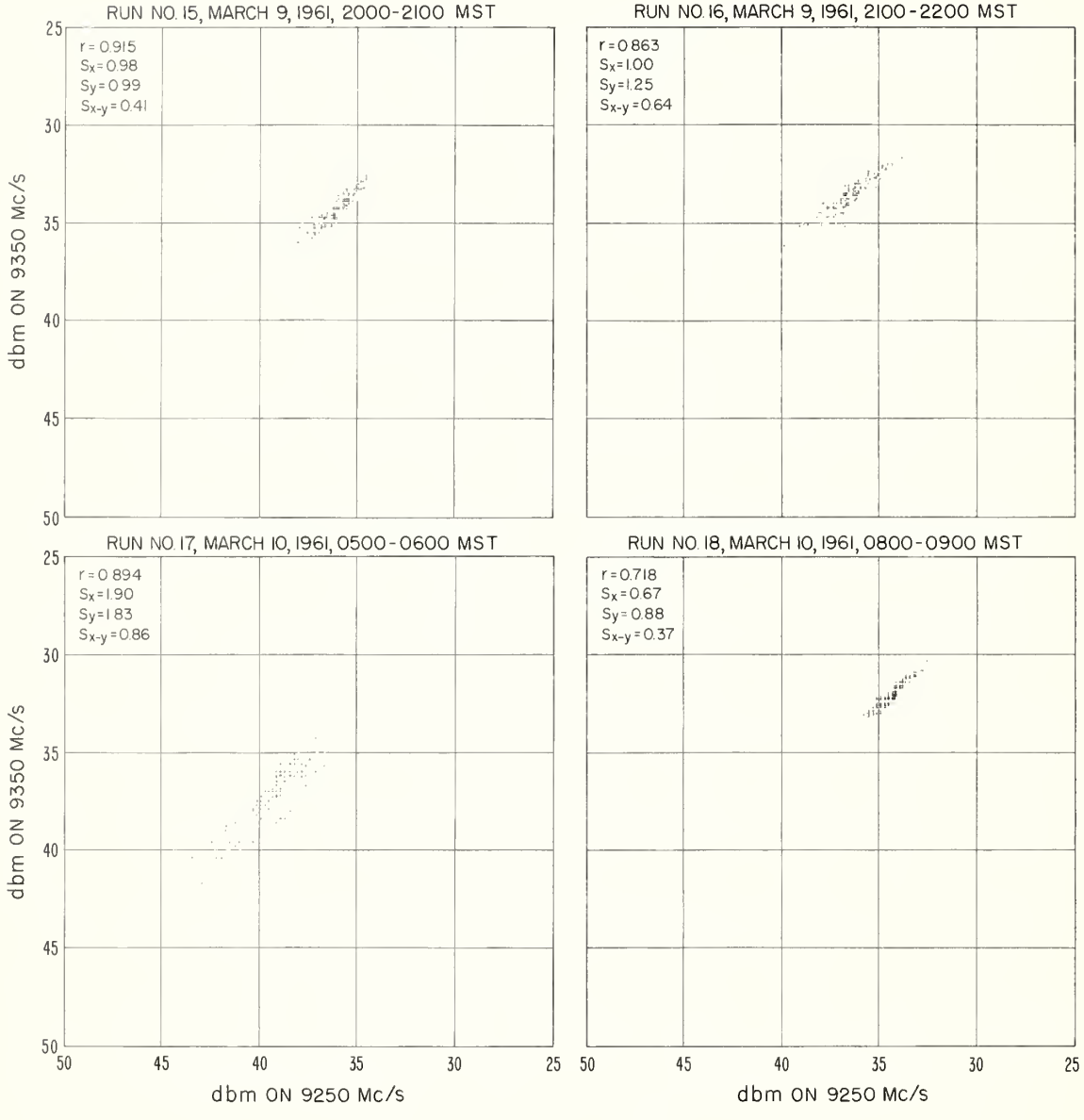

Figure 22

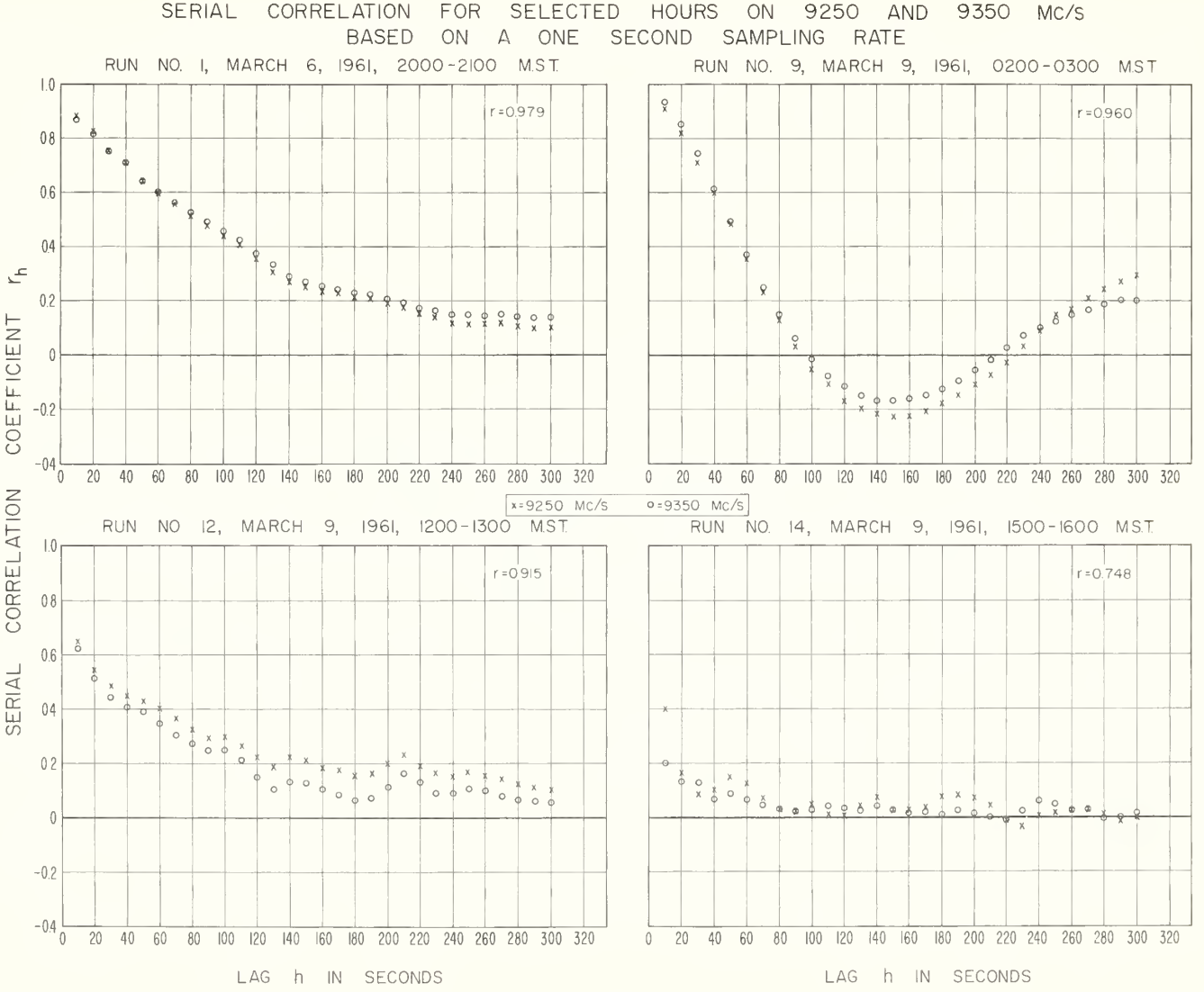
SERIAL CORRELATION FOR SELECTED HOURS ON 9250 AND 9350 Mc/s
BASED ON A ONE SECOND SAMPLING RATE
RUN NO. 1, MARCH 6, 1961, 2000-2100 M.S.T.
r=0.979
RUN NO. 9, MARCH 9, 1961, 0200-0300 M.S.T.
r=0.960
x=9250 Mc/s o=9350 Mc/s
RUN NO 12, MARCH 9, 1961, 1200-1300 M.S.T.
r=0.915
RUN NO. 14, MARCH 9, 1961, 1500-1600 M.S.T.
r=0.748
SERIAL CORRELATION COEFFICIENT r_h
LAG h IN SECONDS
LAG h IN SECONDS

Figure 23

RELATIONSHIP BETWEEN THE CORRELATION COEFFICIENT FOR INSTANTANEOUS VALUES OF TRANSMISSION LOSS ESTIMATED FROM ONE HOUR SETS OF DATA AND ESTIMATION OF THE STANDARD DEVIATIONS OF THE SIGNAL VARIATIONS, s_x, OR THE SIGNAL RATIO VARIATIONS, s_{x-y}.

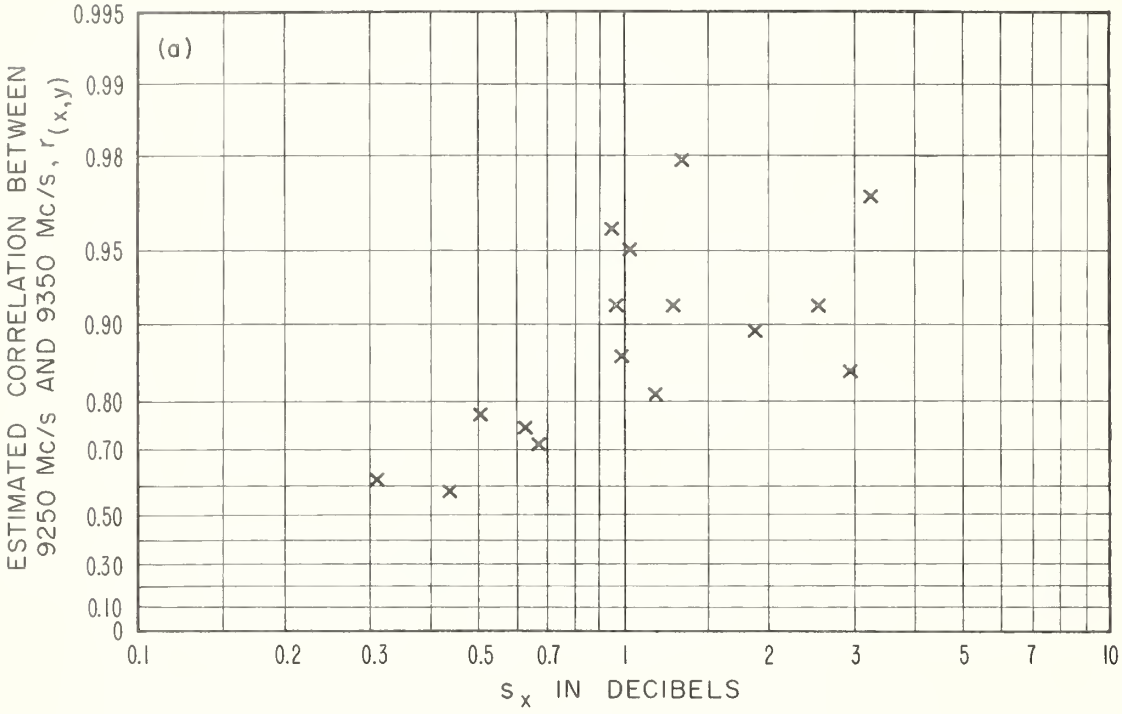

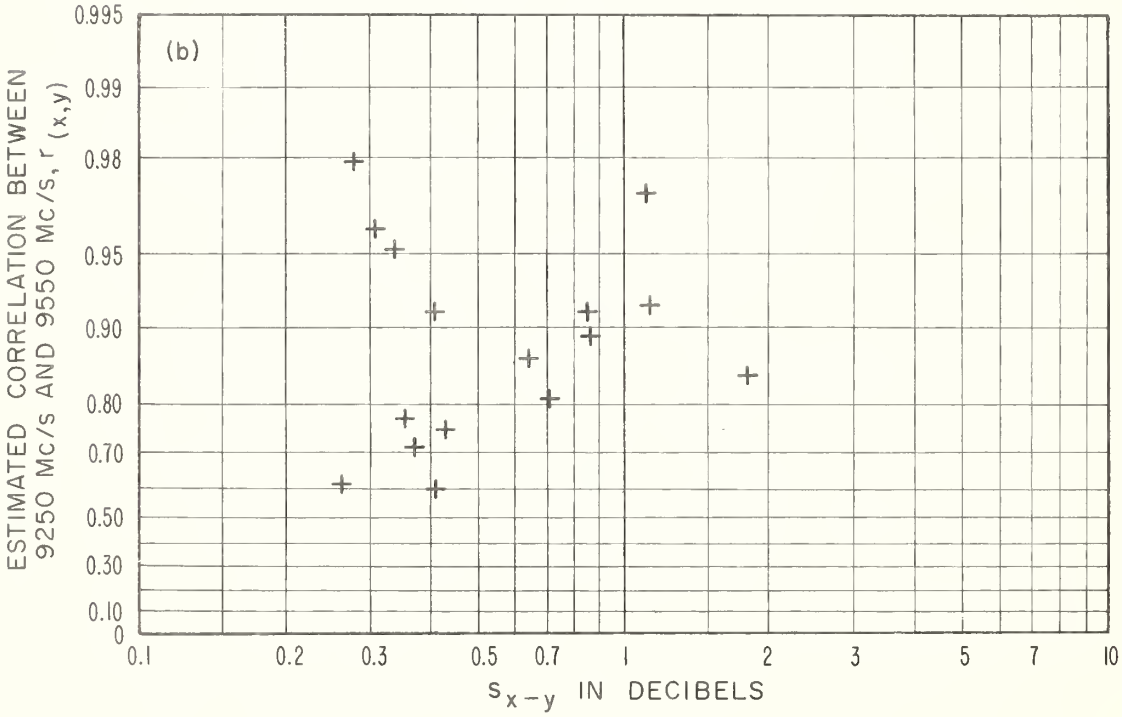

Figure 24

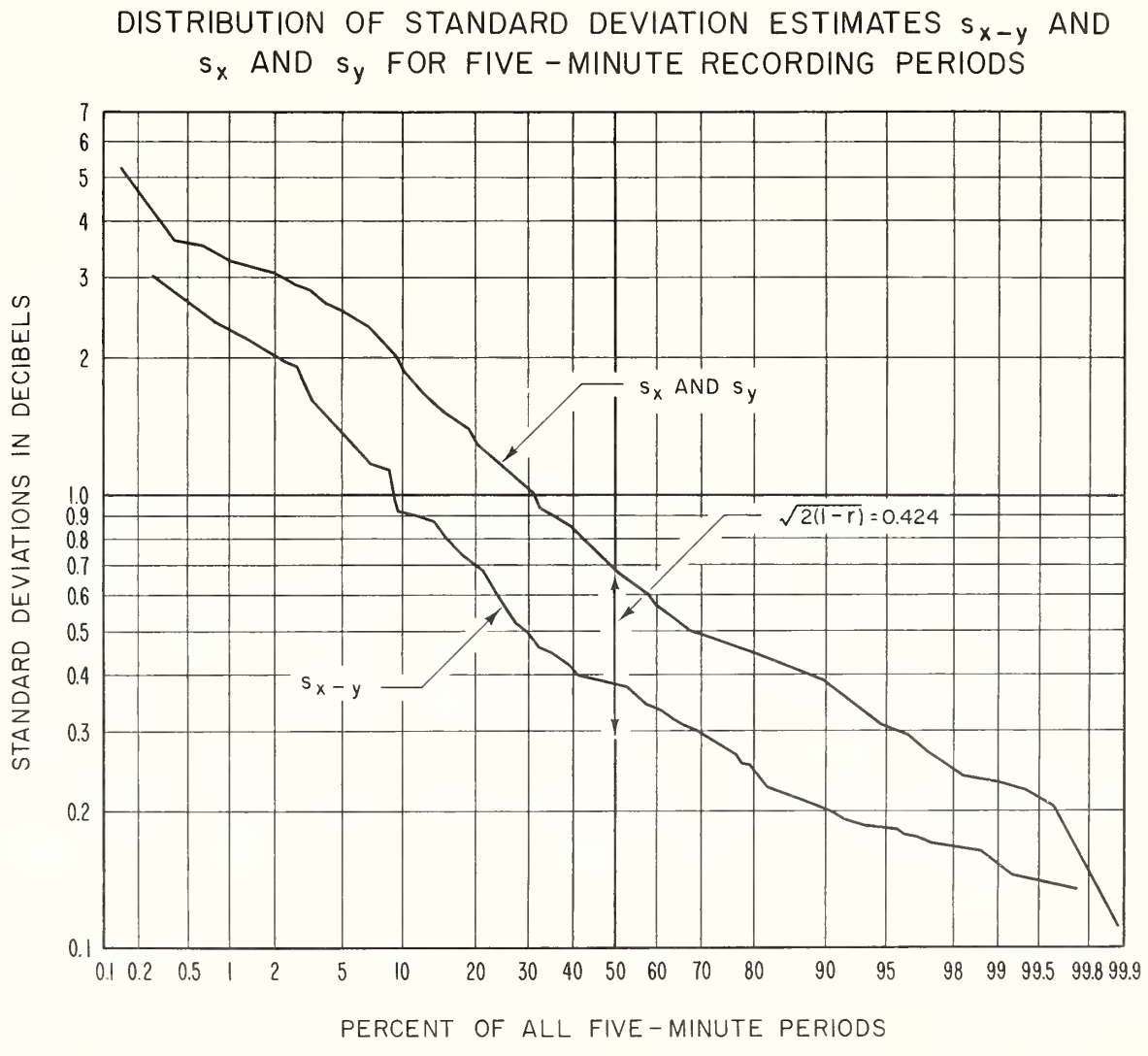
DISTRIBUTION OF STANDARD DEVIATION ESTIMATES s_{x-y} AND s_x AND s_y FOR FIVE-MINUTE RECORDING PERIODS
STANDARD DEVIATIONS IN DECIBELS
7
6
5
4
3
2
1.0
0.9
0.8
0.7
0.6
0.5
0.4
0.3
0.2
0.1
s_x AND s_y
$\sqrt{2(1-r)} = 0.424$
s_{x-y}
0.1 0.2 0.5 1 2 5 10 20 30 40 50 60 70 80 90 95 98 99 99.5 99.8 99.9
PERCENT OF ALL FIVE-MINUTE PERIODS

Figure 25

Department of Commerce
National Bureau of Standards
Boulder Laboratories
Boulder, Colorado

Official Business

NBS

Postage and Fees Paid
U. S. Department of Commerce